AGU PUBLICATIONS

Paleoceanography

RESEARCH ARTICLE
10.1002/2016PA003069

Key Points:
- The boron/calcium proxy is calibrated in *Orbulina universa* for application to ocean acidification during the Paleocene-Eocene Thermal Maximum
- Neither seawater [Ca] nor growth rates affect the proxy; instead, it depends on the ratio of seawater borate/dissolved inorganic carbon or borate/bicarbonate
- Our "Paleocene" calibration can more fully explain the previously measured B/Ca excursion at the Paleocene-Eocene Thermal Maximum

Supporting Information:
- Supporting Information S1
- Table S2
- Table S3
- Table S6

Correspondence to:
L. L. Haynes,
laurah@ldeo.columbia.edu

Citation:
Haynes, L. L., B. Hönisch, K. A. Dyez, K. Holland, Y. Rosenthal, C. R. Fish, A. V. Subhas, and J. W. B. Rae (2017), Calibration of the B/Ca proxy in the planktic foraminifer *Orbulina universa* to Paleocene seawater conditions, *Paleoceanography*, *32*, 580–599, doi:10.1002/2016PA003069.

Received 3 DEC 2016
Accepted 8 MAY 2017
Accepted article online 17 MAY 2017
Published online 17 JUN 2017

Calibration of the B/Ca proxy in the planktic foraminifer *Orbulina universa* to Paleocene seawater conditions

Laura L. Haynes[1,2], Bärbel Hönisch[1,2], Kelsey A. Dyez[1], Kate Holland[3], Yair Rosenthal[4,5], Carina R. Fish[6], Adam V. Subhas[7], and James W. B. Rae[8,9]

[1]Lamont-Doherty Earth Observatory, Columbia University, Palisades, New York, USA, [2]Department of Earth and Environmental Sciences, Columbia University, New York, New York, USA, [3]Research School of Earth Sciences, Australian National University, Canberra, ACT, Australia, [4]Institute for Marine Sciences, Rutgers University, New Brunswick, New Jersey, USA, [5]Department of Earth and Planetary Sciences, Rutgers University, New Brunswick, New Jersey, USA, [6]Department of Earth and Planetary Sciences, University of California, Davis, California, USA, [7]Division of Geological and Planetary Sciences, California Institute of Technology, Pasadena, California, USA, [8]Bristol Isotope Group, University of Bristol, Bristol, UK, [9]Department of Earth and Environmental Sciences, University of St. Andrews, St. Andrews, UK

Abstract The B/Ca ratio of planktic foraminiferal calcite, a proxy for the surface ocean carbonate system, displays large negative excursions during the Paleocene-Eocene Thermal Maximum (PETM, 55.9 Ma), consistent with rapid ocean acidification at that time. However, the B/Ca excursion measured at the PETM exceeds a magnitude that modern pH calibrations can explain. Numerous other controls on the proxy have been suggested, including foraminiferal growth rate and the total concentration of dissolved inorganic carbon (DIC). Here we present new calibrations for B/Ca versus the combined effects of pH and DIC in the symbiont-bearing planktic foraminifer *Orbulina universa*, grown in culture solutions with simulated Paleocene seawater elemental composition (high [Ca], low [Mg], and low total boron concentration ($[B]_T$). We also investigate the isolated effects of low seawater $[B]_T$, high [Ca], reduced symbiont photosynthetic activity, and average shell growth rate on *O. universa* B/Ca in order to further understand the proxy systematics and to determine other possible influences on the PETM records. We find that average shell growth rate does not appear to determine B/Ca in high calcite saturation experiments. In addition, our "Paleocene" calibration shows higher sensitivity than the modern calibration at low $[B(OH)_4^-]$/DIC. Given a large DIC pulse at the PETM, this amplification of the B/Ca response can more fully explain the PETM B/Ca excursion. However, further calibrations with other foraminifer species are needed to determine the range of foraminifer species-specific proxy sensitivities under these conditions for quantitative reconstruction of large carbon cycle perturbations.

1. Introduction

In the surface ocean, the B/Ca ratio of planktic foraminiferal calcite is a promising yet relatively poorly understood proxy for the seawater carbonate system [*Yu et al.*, 2007; *Allen and Hönisch*, 2012; *Babila et al.*, 2014; *Henehan et al.*, 2015; *Salmon et al.*, 2016; *Quintana Krupinski et al.*, 2017]. The B/Ca systematics are based on the pH-dependent speciation of boric acid ($B(OH)_3$) and borate ion ($B(OH)_4^-$) in seawater [e.g., *Hershey et al.*, 1986]. Because increasing pH increases the aqueous concentration of the $B(OH)_4^-$ ion, and because $B(OH)_4^-$ is thought to be the primary species incorporated into marine calcites, boron incorporation increases with higher seawater pH [*Hemming and Hanson*, 1992; *Allen et al.*, 2012]. The incorporation of boron in calcite was proposed by *Hemming and Hanson* [1992] to proceed as follows:

$$CaCO_3 + B(OH)_4^- \leftrightarrow CaHBO_3 + HCO_3^- + H_2O \quad (1)$$

The partition coefficient for this reaction in quantifiable geochemical terms [*Yu et al.*, 2007] then becomes

$$K_D = \frac{B/Ca_{calcite}}{\left[B(OH)_4^-\right]/\left[HCO_3^-\right]_{sw}} \quad (2)$$

Culture experiments with the symbiont-bearing foraminifer species *Orbulina universa*, *Globeriginoides ruber*, and *Trilobatus sacculifer* have shown that B/Ca ratios increase with pH and also decrease with total dissolved inorganic carbon (DIC) in *T. sacculifer* and *O. universa*, with negligible temperature effects and only a minor influence of salinity [*Allen et al.*, 2011; *Allen et al.*, 2012; *Henehan et al.*, 2015; *Howes et al.*, 2017]. In *O. universa*, B/Ca also increases linearly with the total boron concentration ($[B]_T$) of seawater within the range of 1–10×

modern concentrations [*Allen et al.*, 2011]. A recent study by *Howes et al.* [2017] argues that the [$B(OH)_4^-/CO_3^{2-}$] ratio, the [$B(OH)_4^-$/HCO3-] ratio, or [HCO_3^-] are all possible controlling parameters on B/Ca in *O. universa*. However, *Allen et al.* [2012] showed from culture experiments in *T. sacculifer* that while B/Ca increases with [$B(OH)_4^-/CO_3^{2-}$] in variable DIC experiments, it decreases with [$B(OH)_4^-/CO_3^{2-}$] in variable pH experiments (see their Figure 5). This suggests that [$B(OH)_4^-/CO_3^{2-}$] cannot be the controlling parameter on B/Ca. Furthermore, [HCO_3^-] too cannot singularly control B/Ca because when [HCO_3^-] is held constant and [$B(OH)_4^-$] is varied (via $[B]_T$ manipulation), B/Ca increases [*Allen et al.*, 2011]. *Allen et al.* [2012] suggest that because B/Ca increases with [$B(OH)_4^-/HCO_3^-$] in both pH, DIC, and $[B]_T$ experiments, $B(OH)_4^-$ and HCO_3^- (and possibly also CO_3^{2-}) ions likely compete during incorporation, suggesting that the [$B(OH)_4^-$]/DIC ratio of seawater is a more correct controlling parameter. However, in practical terms the effect of using [$B(OH)_4^-/HCO_3^-$] over [$B(OH)_4^-$]/DIC is minimal, as DIC is primarily composed of HCO_3^- at typical seawater pH values [*Allen et al.*, 2012]. These results support the original incorporation hypothesis detailed above [*Hemming and Hanson*, 1992] and suggest that B/Ca should respond to large shifts in surface ocean DIC and/or pH.

However, significant uncertainties about the controls on boron incorporation into marine carbonates, and thus B/Ca, remain [*Allen and Hönisch*, 2012; *Uchikawa et al.*, 2015]. These uncertainties are manifest by discrepancies in the controls on B/Ca in culture [*Allen et al.*, 2011, 2012; *Henehan et al.*, 2015; *Howes et al.*, 2017; *Holland et al.*, 2017], core-tops [*Foster*, 2008; *Yu et al.*, 2007; *Henehan et al.*, 2015; *Quintana Krupinski et al.*, 2017], sediment traps [*Salmon et al.*, 2016; *Babila et al.*, 2014], and inorganic precipitates [*Uchikawa et al.*, 2015; *Gabitov et al.*, 2014; *Ruiz-Agudo et al.*, 2012; *Mavromatis et al.*, 2015]. For example, in sediment trap samples, large seasonal changes in B/Ca of up to 20 μmol/mol have been observed in *G. ruber* without any concurrent significant carbonate chemistry shifts [*Babila et al.*, 2014]. Seasonal light variability has been proposed as the driver for these changes, suggesting a large influence of photosynthesis-driven changes to pH in the foraminiferal microenvironment. Another recent sediment trap study showed that B/Ca is strongly correlated with test thickness in *O. universa*, *G. ruber* (pink), and *G. truncatulinoides*, linking B/Ca in planktic foraminifers to growth rate [*Salmon et al.*, 2016]. Similarly, *Quintana Krupinski et al.* [2017] found that in *G. bulloides* and *Neogloboquadrina incompta*, two symbiont-barren species, the strong covariance of B/Ca with calcite saturation ($\Omega_{calcite}$) indirectly implies a growth rate control. Similar conclusions have been obtained from inorganic $CaCO_3$-precipitation experiments, but the growth rate effect on B/Ca varies in magnitude and sign between studies [e.g., *Uchikawa et al.*, 2015; *Gabitov et al.*, 2014; *Ruiz-Agudo et al.*, 2012]. Recently, it has also been suggested that [PO_4^{3-}] may exert a crystallographic control on planktic foraminiferal B/Ca [*Henehan et al.*, 2015]. These discrepant observations call for detailed investigations of these effects in laboratory culture experiments, where individual parameters can be studied in isolation and across much larger ranges than present in natural seawater.

While a number of confounding factors may obscure B/Ca signals on glacial-interglacial timescales [*Howes et al.*, 2017; *Allen et al.*, 2012], the Paleocene-Eocene Thermal Maximum (PETM) is a climate event that shows great promise for the application of B/Ca. This is because large, consistent B/Ca excursions are observed across this event at multiple geographically disparate sites, suggesting that B/Ca responded to global ocean acidification due to rapid carbon input [*Penman et al.*, 2014; *Babila et al.*, 2016]. Occurring globally at ~55.93 Ma [*Westerhold et al.*, 2009], the PETM is often touted as the closest analog to anthropogenic carbon release and warming [*Zeebe et al.*, 2009], as it is characterized by widespread dissolution of seafloor carbonates, a large negative carbon isotope excursion, pronounced warming, and planktic foraminiferal B/Ca and $\delta^{11}B$ excursions [*Zachos et al.*, 2005; *Penman et al.*, 2014; *Babila et al.*, 2016]. These geochemical records suggest extreme ocean acidification, with an intensity that is larger than estimated from models [*Penman et al.*, 2014; *Babila et al.*, 2016]. Furthermore, the ~25–40 μmol/mol B/Ca decrease observed across the interval, measured in the now-extinct species *Morozovella velascoensis*, is larger than can be predicted from a simple pH control on the proxy using modern seawater calibrations. Specifically, when modern culture calibrations for *O. universa* and *T. sacculifer* [*Allen et al.*, 2012] are used to interpret the B/Ca data of *Penman et al.* [2014] in terms of peak-PETM [$B(OH)_4^-$]/DIC, the size of the B/Ca excursion translates to negative [$B(OH)_4^-$]/DIC ratios for the PETM (Figure 1a). Only the calibration slopes of *G. ruber* [*Allen et al.*, 2012; *Henehan et al.*, 2015] give a positive ratio, but the strong nonlinearity of this calibration at the low pH end in *G. ruber* (pink) (Figure S1 in the supporting information), as well as the much higher values in this species compared to *M. velascoensis*, lends low confidence to this interpretation.

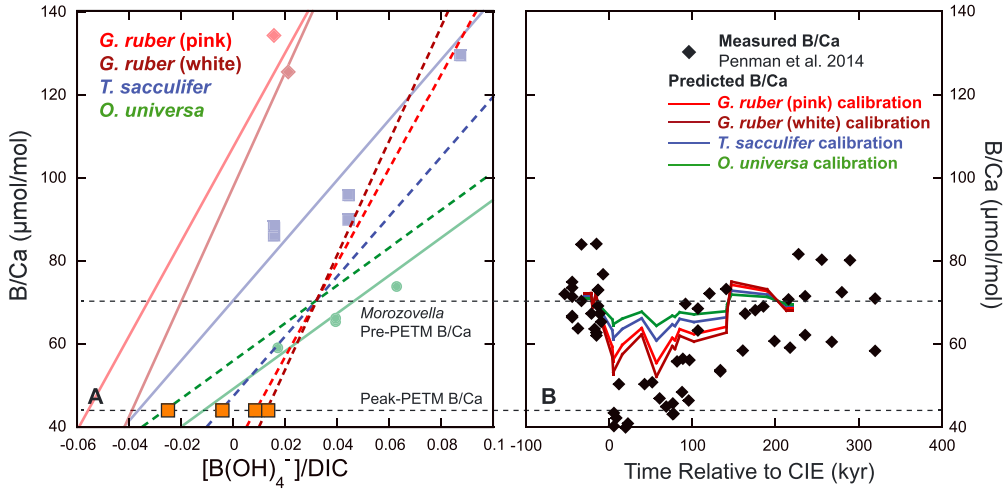

Figure 1. Modern B/Ca proxy calibrations are not applicable to the PETM B/Ca excursion. (a) Calibrations for B/Ca versus pH in *G. ruber* (white [*Henehan et al.*, 2015] and pink [*Allen et al.*, 2012]), *T. sacculifer* [*Allen et al.*, 2012], and *O. universa* [*Allen et al.*, 2011] are shown (solid colored lines and symbols). The horizontal dashed black lines indicate average pre-PETM and peak-PETM B/Ca ratios from the *M. velascoensis* study of *Penman et al.* [2014] (black diamonds). When the calibrations of *T. sacculifer* and *O. universa* are shifted through the pre-PETM B/Ca average (dotted lines), negative seawater $[B(OH)_4^-]$/DIC ratios are predicted at the peak-PETM (orange squares). (b) The predicted B/Ca shift resulting from the ~0.3 unit pH decline estimated from boron isotope measurements across the PETM [*Penman et al.*, 2014]. The colored lines show the proportion of the B/Ca excursion that each calibration can explain.

The inability for modern calibrations to explain the PETM excursion is further highlighted in Figure 1b. If the δ^{11}B-derived pH excursion of −0.3 units [*Penman et al.*, 2014] is paired with modern B/Ca culture calibrations to predict the B/Ca excursion, the result merely encompasses a small portion of the observed B/Ca decrease. This inability to produce coherent peak-PETM $[B(OH)_4^-]$/DIC estimates indicates that either (a) modern calibrations for pH are not appropriate and we thus cannot extrapolate them to interpret the PETM data or (B) there are additional controls on B/Ca, such as total DIC or symbiont photosynthesis, that changed drastically over the PETM. A significant DIC increase at the PETM has been suggested from the coupled ocean-sediment model Long-term Ocean-atmosphere-Sediment CArbon cycle Reservoir (LOSCAR), which *Komar and Zeebe* [2011] parameterized with the combined effects of carbon injection, seafloor $CaCO_3$ dissolution, and terrestrial weathering influxes to estimate a total DIC increase of ~350 µmol kg^{-1}. Given that foraminiferal B/Ca decreases with increasing DIC [*Allen et al.*, 2012, *Howes et al.*, 2017, *Holland et al.*, 2017], we hypothesize that the DIC pulse at the PETM could have contributed significantly to the B/Ca excursion.

Modern calibrations may not be applicable to the PETM for a couple of reasons. First, calibration experiments have not yet been conducted below a $[B(OH)_4^-]$/DIC of about 0.015–0.017 [*Allen et al.*, 2012]. Given that the Paleocene ocean likely had a low surface ocean pH [*Penman et al.*, 2014; *Anagnostou et al.*, 2016] and lower $[B]_T$ than the modern ocean [*Lemarchand et al.*, 2000], peak-PETM conditions were likely characterized by very low $[B(OH)_4^-]$/DIC. Second, it has been suggested that the major and trace element chemistry of the ocean were significantly different during the Paleocene compared to today [*Lemarchand et al.*, 2000; *Lowenstein et al.*, 2014]. Specifically, it has been proposed that the total boron concentration ($[B]_T$) of seawater was about 10% lower in comparison to today [*Lemarchand et al.*, 2000] and that the [Ca] of seawater was twice as high [*Lowenstein et al.*, 2014]. Because B/Ca in *O. universa* increases with the $[B]_T$ of seawater [*Allen et al.*, 2011], one would expect lower B/Ca at lower than modern $[B]_T$, but experimental evidence for this hypothesis was hitherto missing as experiments at low $[B]_T$ had yet to be conducted. In addition, the relationship between foraminiferal B/Ca and pH needs to be empirically calibrated at lower $[B]_T$, as well as at estimated "Paleocene" seawater Mg/Ca (Mg/Ca_{sw} = 1.5 mol/mol [*Lowenstein et al.*, 2014]). It is conceivable that low seawater Mg/Ca could have an impact on the sensitivity of B/Ca to pH and DIC if the mechanism for delivery of ions to the site of calcification proceeds differently under low Mg/Ca. For example, reduced $[Mg^{2+}]$ may have an effect on the requirements for ion concentration to promote calcification. Mg^{2+} is an inhibitor to calcite formation [*Mucci and Morse*, 1984], and it has been hypothesized that significant H^+ removal, or pH

up-regulation, is the more energy-efficient method to overcome this barrier to precipitation [*Zeebe and Sanyal*, 2002]. If regulation of the internal calcifying environment through H^+ removal is less necessary under low Mg/Ca_{sw}, then this could also affect the relationship of foraminiferal B/Ca to seawater-pH.

Additional concerns arise from the fact that the PETM species *M. velascoensis* is now extinct [*Kelly et al.*, 2001] and thus cannot be calibrated empirically. However, the $\delta^{13}C$ signature of this species increases with test size, suggesting that *M. velascoensis* was symbiont-bearing and thus confined to the surface ocean [*D'Hondt et al.*, 1994], where it should have recorded surface ocean acidification similar to modern species. *Edgar et al.* [2013] found that foraminifers likely lost their symbionts and "bleached" across the Middle Eocene Climatic Optimum, as recorded in the reduction of the $\delta^{13}C$/size pattern at this time. Whereas a similar reduction has not yet been observed at the PETM [*Babila et al.*, 2016], it is critical to assess the degree to which modifications in symbiont activity could affect B/Ca.

While *M. velascoensis* is now extinct, we can approximate the Paleocene B/Ca systematics with culture studies of modern planktic foraminifera. Here we report a series of experiments with *O. universa*, a symbiont-bearing planktic foraminifer, which we grew under simulated Paleocene seawater conditions (Table 1). We specifically calibrated B/Ca to changing pH and DIC at constant high [Ca], low [Mg], and low $[B]_T$. We also investigated the isolated effects of both low $[B]_T$ and high [Ca] in otherwise ambient seawater chemistry to further understand how these isolated changes in seawater chemistry affect B/Ca. In addition, we examine how B/Ca is affected by the decreased symbiont activity that occurs under low-light conditions [*Rink et al.*, 1998] to further assess the parameters that control B/Ca in natural ocean samples and the potential effects of symbiont "bleaching." To assess a growth rate control on B/Ca, we estimate average shell growth rates in our cultured foraminifers from final shell size and weight data in each experiment. Finally, we apply our new Paleocene calibrations to B/Ca data from Ocean Drilling Program (ODP) Site 1209 on Shatsky Rise [*Penman et al.*, 2014] to estimate the ability of our Paleocene calibrations to explain the measured B/Ca excursion across the PETM.

2. Methods

2.1. Culturing Methods

Culturing experiments were carried out at the Wrigley Institute for Environmental Studies on Santa Catalina Island in the summer of 2013 and at the Isla Magueyes Marine Science Laboratory in La Parguera, Puerto Rico (PR) in the spring of 2010 and 2015. Juvenile *O. universa* were hand-collected by scuba divers 2 km NNE of Santa Catalina Island and 15 km offshore of Isla Magueyes at a water depth of 2–8 m. Specimens were identified and measured using light microscopes and were then transferred into 120 mL soda-lime glass jars filled with experimental seawaters. Jars were sealed with Parafilm® and tight-fitting lids to limit CO_2 exchange with the atmosphere. Foraminifers were hand-fed a 1 day old *Artemia* nauplius every 2 days.

In $[B]_T$ and Paleocene carbonate chemistry experiments, experimental seawaters were composed of 50% natural and 50% artificial seawater (filtered using 0.8 μm nitrate cellulose filters). Culture water concentrations of [Ca], [Mg], and $[B]_T$ were manipulated to reach estimated Paleocene values (20 mmol/kg, 30 mmol/kg, and 365 μmol kg^{-1}, respectively, at a salinity of 33.1–33.3; Table 1) [*Lowenstein et al.*, 2014, *Lemarchand et al.*, 2000]. In boron concentration experiments, $[B]_T$ was manipulated to reach 0.5, 1.5, and 2× modern values (where modern $[B]_T$ = 432.6 μmol kg^{-1} at S = 35 [*Lee et al.*, 2010]) via the addition of boric acid. DIC was varied independently from pH by the addition of $NaHCO_3$ to reach target values ranging from 1000 to 4000 μmol kg^{-1}. pH was then altered by the titration of seawater batches with NaOH or HCl to respectively raise or lower pH to target values on the total scale (pH_{Tot}). In addition, no nutrients were added to artificial seawater experiments, so that $[PO_4^{3-}]$ and $[NO_3^-]$ were reduced compared to ambient conditions. All experiments from Catalina were conducted at a controlled temperature of 21.6 or 21.9°C ± 0.1°C (1σ; Table S2 in the supporting information). In all experiments, a 12–12 h light-dark diurnal cycle was maintained using Osram Lumilux T5 skywhite high output bulbs. Photosynthetic active radiation intensities were measured using a light meter every 7–10 days. Low-light experiments were conducted in natural filtered seawater on both Catalina Island and in Puerto Rico (2015), where light levels were kept at a constant 19 μmol photons m^{-2} s^{-1} (compared to high-light conditions, 319 ± 28 μmol photons m^{-2} s^{-1} in PR, 291 ± 36 μmol photons m^{-2} s^{-1} on Catalina, 1σ). In [Ca] experiments from 2015, which were also conducted in Puerto Rico, $CaCl_2 \cdot 6H_2O$ was added to ambient seawater to reach target concentrations of 15 and

AGU Paleoceanography

10.1002/2016PA003069

Table 1. Experimental Seawater and Foraminiferal Trace Element Data[a]

Exp. No.	pH Total	2σ	Alkalinity (μmol/kg)	2σ	DIC (μmol/kg)	2σ	Ω Calcite	2σ	$[B(OH)_4^-]$/DIC	PAR[b]	$[B]_T$ (μmol/kg)	[Ca] (mMol/kg)	[Mg] (mMol/kg)	B/Ca (μmol/mol)	2σ	Mg/Ca (mmol/mol)	2σ
DIC Experiment																	
LH3a	7.75	0.06	1069	22	**998**	25	2.3	0.3	0.0398	291	367	18.5	28.2	90.4	6.0	-	
LH3b														85.4	5.6	-	
LH2a	7.84	0.06	2197	14	**2063**	28	5.8	0.8	0.0226	291	361	18.9	28.2	44.2	2.9	-	
LH2b														52.6	3.5	-	
LH4a	7.78	0.04	3143	30	**2998**	36	7.3	0.8	0.0141	291	367	18.6	28.8	49.9	3.3	-	
LH4b														49.8	3.3	-	
LH5a	7.81	0.06	4156	96	**3970**	99	9.9	1.5	0.0108	291	359	18.2	27.9	36.4	2.4	-	
LH5b														44.7	2.9	-	
LH5c														45.1	3.0	-	
pH/DIC Experiment																	
LH6	**7.53**	0.04	2031	40	**2000**	42	2.7	0.3	0.0120	291	359	18.3	28.1	48.3	3.2	-	
LH7	**7.89**	0.03	2156	14	**2005**	20	6.1	0.5	0.0258	291	365	18.6	28.5	62.6	4.1	-	
LH11a	**8.24**	0.02	2371	30	**2034**	30	12.8	0.5	0.0478	291	364	18.4	28.3	74.3	4.9	-	
LH11b														70.6	4.7	-	
LH8	**7.54**	0.06	3035	26	**3000**	33	4.0	0.6	0.0079	291	348	17.7	27.3	43.7	2.9	-	
LH9a	**7.89**	0.08	3213	14	**3016**	47	9.1	1.7	0.0169	291	359	18.2	28.0	53.4	3.5	-	
LH9b														55.2	3.6	-	
$[B]_T$ Experiment																	
LH13a	7.93	0.05	2179	36	2022	39	3.4	0.4	0.0161	291	**207**	9.6	50.7	27.4	1.8	-	
LH13b														30.0	2.0	-	
LH14	7.95	0.03	2247	8	2016	21	3.6	0.3	0.0654	291	**596**	9.7	51.0	101.7	6.7	-	
LH15a	7.94	0.04	2291	16	2025	27	3.6	0.3	0.0651	291	**812**	9.9	52.4	171.8	11.3	-	
LH15b														163.6	10.8	-	
Low Light Experiment																	
LH16a[c]	7.98	0.05	2235	8	2019	29	3.9	0.4	0.0343	**19**	397	9.8	51.2	66.0	4.4	8.80	0.07
LH16b[c]														65.4	4.3	9.93	0.08
BH1a[d]	8.04	0.06	2365	16	2040	47	5.4	0.7	0.0471	**19**	427	10.1	55.5	57.3	3.8	8.18	0.07
BH1b[d]														58.7	3.9	8.55	0.07
[Ca] Experiment																	
KD1a	8.03	0.05	2404	18	2052	38	9.1	0.9	0.0470	320	424	**20.8**	54.0	63.1	4.2	-	
KD1b														75.8	5.0	-	
KD2a	8.02	0.03	2393	16	2066	28	7.1	0.5	0.0455	320	429	**15.8**	54.3	78.7	5.2	-	
KD2b														82.8	5.5	-	
BH6a	8.03	0.03	2364	16	2046	25	5.3	0.3	0.0460	320	428	**10.8**	54.3	70.5	4.7	7.64	0.06
BH6b														72.1	4.8	7.87	0.06
BH6c														68.4	4.5	6.84	0.05

[a]Values in boldface denote variable changed in each experiment.
[b]In μmol photons/m^2/s.
[c]Experiment conducted on Santa Catalina Island.
[d]Experiment conducted in Puerto Rico.

20 mmol/kg seawater (in comparison to ~10 mmol/kg seawater at ambient conditions). In this [Ca] experiment matrix, temperature was kept constant at 25.9°C± 0.1°C and salinity ranged from 36.5 to 37.5 (Table 1). This large range is due to the addition of $CaCl_2$ salt to increase [Ca].

Alkalinity and pH of experimental seawaters were measured at 25°C on a Metrohm titrator at the beginning and end of each experiment to investigate CO_2 invasion or outgassing during feeding. Foraminifers that underwent gametogenesis were removed from culture waters, measured, and stored for analysis. In the low-light experiment one foraminifer was erroneously added that was terminated before gametogenesis (hereafter abbreviated as "terminated"). However, we estimate that the weight added from this individual likely comprised <5% of the total sample weight (see the supporting information), equivalent to the amount assumed to be contributed by juvenile calcite [*Spero and Parker*, 1985], and we do not expect this to significantly bias our results. However, in order to investigate the potential effects of terminated foraminifer calcite on trace elements, we made replicates from one experiment (BH7) of both gametogenic and terminated foraminifers (see Table S4 and Figure S2 in the supporting information). The number of foraminifers included in each sample ranged from 2 to 22 (Table S2). Where shell material was readily abundant, replicates were made based on size fraction (Table S2).

Carbonate system parameters were calculated using a CO2SYS.m MATLAB script modified after *Van Heuven* [2011] (See supporting information) to allow for the influence of altered seawater chemistry on the carbonate system, including $[B]_T$, [Ca], and [Mg]. The influence of [Ca] and [Mg] on K_1, K_2, and KSO_4 equilibrium constants was calculated using the Python script PyMyAMI from *Hain et al.* [2015], incorporated into the MATLAB script. Calculations also include conversion of pH from the National Bureau of Standards (NBS) scale (measured) to the total scale at the appropriate experimental and analysis temperatures. Carbonate system data from *Allen et al.* [2011] were also recalculated using the above constants and seawater $[B]_T$ of *Lee et al.* [2010] for accurate comparison (Table S2). The uncertainty in carbonate system parameters resulting from the measured uncertainties associated with *T*, *S*, pH, and alkalinity was estimated using a Monte Carlo simulation of these variables and their normally distributed uncertainties in the CO2SYS.m program (N = 10,000 iterations). The 2σ values on calculated parameters are reported in Table 1.

2.2. Analytical Methods

Samples were cleaned and prepared for analysis according to the same methods as *Allen et al.* [2012]. Briefly, samples were weighed, cracked, and transferred to acid cleaned vials. If enough $CaCO_3$ material was present after cracking, samples were homogenized and subsequently split manually with a brush to create replicates of roughly equal weight (in addition to the size fraction replicates described above, see Table S2). In a boron-free laminar flow bench splits were rinsed 3× with ultrapure B-filtered Milli-Q water, followed by oxidation in a buffered hydrogen peroxide solution (equal parts 0.1 N NaOH +30% H_2O_2) at 70–80°C for two 30 minute periods. Samples were then rinsed again 3× with Milli-Q water, transferred to clean vials with a severed pipette tip, and leached with 0.001 N HNO_3 to remove adsorbed ions. Finally, samples were rinsed 3× with Milli-Q and left to dry. After cleaning, material was transferred to create more even sample weights between replicates for two of our DIC experiments (LH2 and LH5; Table 1). B/Ca and Mg/Ca were measured at Rutgers University using a Thermo Finnigan Element XR sector field inductively coupled plasma–mass spectrometer (ICP-MS) operated in low resolution ($m/\Delta m$ = 300) following a modified protocol of *Rosenthal et al.* [1999] in which anhydrous ammonia gas was injected into a quartz cyclonic spray chamber to elevate the pH of the injected sample to >9.14. This modification reduces the boron memory effect and improves washout efficiency [*Al-Ammar et al.*, 2000]. Prior to analysis, samples were dissolved using 0.065 N HNO_3 and diluted with 0.5 N HNO_3 to achieve final Ca concentrations of 2–6 mM to minimize matrix effects. Additionally, a [Ca] solution of 1.5–8 mM was run to quantify and correct for matrix effects; all corrections were <1%. Long-term 2 relative standard deviation precision on B/Ca and Mg/Ca measurements is 6.6% and 0.8%, respectively.

Experimental seawaters were sampled immediately before and after culturing, filtered into an acid-cleaned 15 mL PTFE vial with a 0.2 μm syringe filter, acidified with 150 μL Optima grade HNO_3, covered with Parafilm, and stored until analysis at the Australian Natural University in the spring of 2014 (Catalina) and summer of 2015 (Puerto Rico). All seawater elemental compositions were determined via simultaneous ICP-atomic emission spectrometry (Varian Vista Pro Axial). Prior to analysis, samples were diluted 10× with 2% HNO_3 and then run using a standard-sample bracketing routine with a synthetic seawater standard of

known elemental concentrations. Initial and final seawater $[B]_T$, [Mg], and [Ca] values were averaged to determine experimental values (Table 1).

To compare our B/Ca analyses with those conducted at Cambridge University [*Allen et al.*, 2011], the latter values were corrected for interlaboratory biases using the following equation from *Allen et al.* [2012]:

$$B/Ca_{Rutgers} = 1.085 \times B/Ca_{Cambridge} - 1.09 \quad (3)$$

2.3. Estimation of Average Shell Growth Rates

While we did not directly measure instantaneous shell growth rates in this study, we estimate average shell growth rate in each experiment based on final shell weight, size, and duration of sphere thickening data for foraminifers where each data parameter is available (Table S2). Individual shell weights were measured in microgram, and the timing of the onset of spherical chamber formation in our cultured *O. universa* was noted and used as the growth period time constraint to find relative rates in $\mu g\ d^{-1}$ [as in *Allen et al.*, 2016]. Because the contribution of juvenile calcite to the total shell weight is presumed to be minimal [*Spero and Parker*, 1985], we assume major growth only during sphere formation and thickening. To convert growth rates to area-normalized rates (in $\log_{10}$ mol calcite $m^{-2}\ sec^{-1}$) for comparison of average values to inorganic calcite growth rates [*Uchikawa et al.*, 2015], we converted estimates in $\mu g\ d^{-1}$ to mol s^{-1} after *Allen et al.* [2016]. The surface area of each sphere was estimated using gas adsorption surface area measurements (i.e., the Brunauer-Emmett-Teller (BET) method [*Brunauer et al.*, 1938]) of pooled *O. universa* shells made in 425–515, 515–600, and 600–865 μm size classes (see Table S2 for the calculation details). *Allen et al.* [2016] used surface area measurements from bulk marine sediment samples [*Gehlen et al.*, 2005] to estimate cultured foraminifera shell surface area; however, the mono-specific measurements of fossil *O. universa* shells that we use here are likely more accurate. These estimates were then used to normalize growth rates to surface area, yielding estimates in mol $m^{-2}\ s^{-1}$. For samples where replicates were made based on size class instead of being split from a homogeneous pool of shells, growth rate estimates were made for each replicate based on the data from individuals added to each sample.

3. Results

3.1. Estimated Foraminiferal Growth Rates

Average foraminifer shell weights were lowest in the low DIC experiment (28 ± 11 μg) and were highest (>100 μg) in four specimens that spent an exceptionally long time in culture (>24 days, shells from LH3a and LH9a; Table S2, not shown in Figure 2). Excluding these unusual long-living specimens, the upper range for average shell weight is ~67 μg, observed in the high DIC and high [Ca] experiments (Figure 2). Growth rates in $\mu g\ d^{-1}$ are also low in the low-DIC experiment, as well as the low-light experiment from Catalina (4.8 ± 1.4 and 4.7 ± 1.1 $\mu g\ d^{-1}$, respectively). From DIC = 1000–4000 μmol/kg, growth rate increases 1.6-fold, consistent with the ~doubling observed by *Holland et al.* [2017] across a similar DIC range. The highest growth rates are observed in foraminifers from the PR culture season (8.1–11.5 $\mu g\ d^{-1}$), as well as at high pH (9.0 ± 1.5 $\mu g\ d^{-1}$). These rates are similar to those found by *Allen et al.* [2016] in *O. universa* (6.0 $\mu g\ d^{-1}$ on average). However, growth rate only reached 7.5 $\mu g\ d^{-1}$ in that study at high pH, where $[CO_3^{2-}]$ = 300 $\mu mol\ kg^{-1}$, compared to values of up to 9.0 $\mu g\ d^{-1}$ in our high pH experiments where $[CO_3^{2-}]$ was lower (240 $\mu mol\ kg^{-1}$). This could indicate that the enhanced [Ca] in our experiments promoted more rapid growth or enhanced gametogenic calcite formation at similar $[CO_3^{2-}]$. When BET surface area estimates are used to calculate net area-normalized growth rate, growth rate estimates have an average value of −8.49 ± 0.12, reported in units of $\log_{10}$ rate mol $m^{-2}\ s^{-1}$, across all experiments.

3.2. Effects of Using Foraminifers That Did Not Undergo Gametogenesis

In order to investigate any potential biases of using foraminifers that were terminated prior to gametogenesis on trace element/Ca ratios, we compared results from gametogenic and terminated foraminifers in an experiment from Puerto Rico. We found a significant increase in both B/Ca (from 74 to 91 μmol/mol) and Mg/Ca (from 8.2 to 11.7 mmol/mol) in terminated foraminifers compared to gametogenic specimens (Figure S2 and Table S4). Whereas we do not estimate that this significantly biased our low-light samples, as we added only one terminated specimen to 18 gametogenic foraminifers, this highlights that using a significant

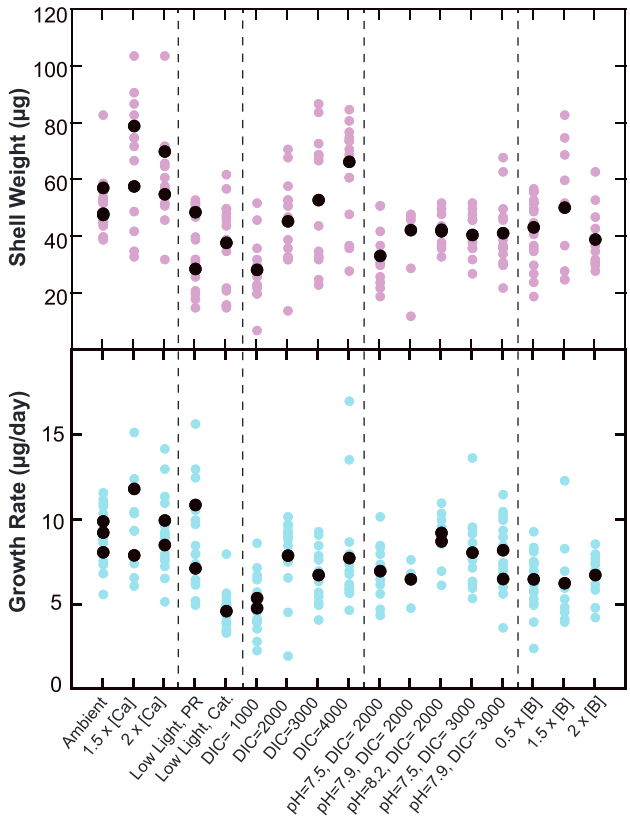

Figure 2. Shell weight (µg) and estimates of foraminiferal growth rate (µg d^{-1}). The mean experimental values are show in black, while individual shell estimates of weight and growth rate are shown in purple and blue, respectively. If replicates were made based on size fraction, the average from each replicate is shown.

fraction of foraminifers that do not undergo gametogenesis can bias bulk trace element analyses (section S2 in the supporting information).

3.3. Isolated Variables $[B]_T$, Low Light, and [Ca]

We investigated the effects of low $[B]_T$ on B/Ca in *O. universa* shells at the paleoceanographically relevant values of 0.5, 1.5, and 2× modern concentrations. B/Ca responds linearly to changing $[B]_T$ in agreement with experiments at 5× and 10× modern $[B]_T$ [*Allen et al.*, 2011] (Figure 3a). B/Ca in *O. universa* thus responds to the $[B(OH)_4^-]$ of seawater across the range of 0.5–10× modern concentrations by the following linear equation, taking into account uncertainty in measured B/Ca and $[B(OH)_4^-]$:

$$\mathrm{B/Ca}\ (\mu\mathrm{mol/mol}) = 1.38{\pm}0.09 \times \left[\mathrm{B(OH)_4^-}\right]\ (\mu\mathrm{mol\ kg^{-1}}) - 23{\pm}6\ \left(R^2 = 0.999\right) \quad (4)$$

Because the highest $[B]_T$ experiments have the largest relative B/Ca uncertainty, the regression is weighted toward the lower $[B]_T$ experiments and thus shows a better fit at low $[B(OH)_4^-]$ (Figure 3a). The 95% confidence intervals on this regression show that the regression intercept is within uncertainty of the origin. Our data agree within uncertainty with the data of *Howes et al.* [2017], where $[B]_T$ = 10× and B/Ca was measured via laser ablation (Figure 3a).

In response to seawater [Ca], B/Ca does not show a significant change over our studied range of 10–20 mmol/kg (Figure 3b). Because the salinity of high [Ca] experiments was elevated due to the addition of $CaCl_2$ salt, we normalize B/Ca in these experiments to S = 35 using the B/Ca-salinity relationship of *Allen et al.* [2012], which does not change the observed trend in B/Ca (Figure 3b and Table S2). Low-light experiments on Santa Catalina Island at 19 µmol photons m^{-2} s^{-1} yielded B/Ca ratios of 66 ± 4 µmol/mol, which is not significantly different from high-light experiments (65 ± 4 µmol/mol [*Allen et al.*, 2011] where light intensity was set at 406 ± 108 µmol photons m^{-2} s^{-1}; Figure 3c). However, B/Ca was significantly lower in low-light experiments from Puerto Rico (58 ± 4 µmol/mol) compared to an "ambient" experiment

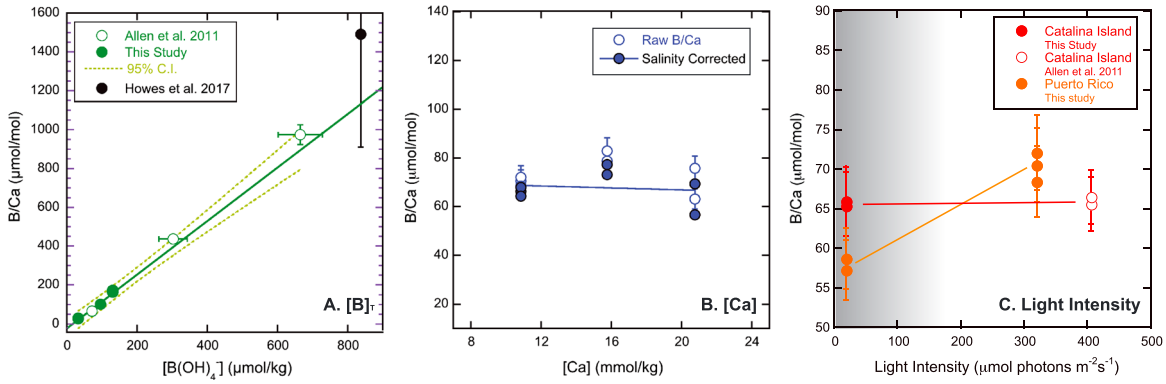

Figure 3. Effects of $[B]_T$, [Ca], and light intensity on B/Ca in *O. universa*. (a) $[B]_T$ experiments from this study (filled green circles) those of *Allen et al.* [2011] (open green circles) and the DIC = 2236 μmol kg^{-1} experiment of *Howes et al.* [2017] (black circle) are shown versus $[B(OH)_4^-]$. The linear regression does not include the *Howes et al.* [2017] data given that DIC was higher in this experiment and the uncertainty bounds are large (their 2 SE is plotted here). (b) B/Ca in *O. universa* does not respond to elevated [Ca]. Raw data are shown in open circles; B/Ca normalized to S = 35 is shown in filled circles. (c) The effect of light intensity on B/Ca from experiments on both Santa Catalina Island (red circles) and Puerto Rico (orange circles) is shown. Note that the B/Ca scale (*y* axis) changes between panels. The 2σ errors on culture data are shown.

(70 ± 5 μmol/mol) from the same culture season. Salinity was not significantly different between low-light and high-light experiments, so no salinity corrections have been applied to the data.

3.4. Paleocene Carbonate Chemistry Experiments

In general, *O. universa* specimens grown under Paleocene seawater conditions have similar B/Ca ratios as those grown in "modern" seawater (Figure 4). The trends observed in our Paleocene carbonate chemistry experiments are also consistent with those carried out previously in modern seawater [*Allen et al.*, 2011, 2012; *Henehan et al.*, 2015] in which B/Ca increases with pH and decreases with total DIC. When DIC is increased across a range of 1000–4000 μmol kg^{-1} (holding $[B(OH)_4^-]$ constant), B/Ca ratios decrease from 88 ± 6 to 42 ± 3 μmol/mol (Figure 4a). In order to assess the effects of changing pH and DIC in concert, we varied $pH_{(Tot)}$ over the range of 7.5–8.3 and 7.5–7.9 at set DIC values of 2000 (considered ambient) and 3000 μmol kg^{-1}, respectively. B/Ca increases with pH from 48 ± 3 to 73 ± 5 μmol/mol at a DIC of 2000 μmol kg^{-1} and from 44 ± 3 to 54 ± 4 μmol/mol at a DIC of 3000 μmol kg^{-1} (Figure 4c).

4. Discussion

4.1. Effects of Variable $[B]_T$

In our $[B]_T$ experiments (0.5, 1.5, and 2× modern $[B]_T$), B/Ca decreases linearly toward zero at low $[B(OH)_4^-]$ and follows the same linear relationship of the high $[B]_T$ experiments of *Allen et al.* [2012] (Figure 3a). This suggests that Paleocene foraminifers living in seawater with lower $[B]_T$ than in the modern ocean would record overall lower B/Ca ratios. Paleocene *M. velascoensis* recorded B/Ca ratios clustering around 60–70 μmol/mol before the PETM carbon system perturbation, reaching values as low as 30 μmol/mol during peak acidification [*Babila et al.*, 2016; *Penman et al.*, 2014]. *Babila et al.* [2016] note that this is much lower than analogous modern surface dwelling species such as *T. sacculifer* and *G. ruber*, which typically record B/Ca ~90–140 μmol/mol. The lower $[B]_T$ of the surface ocean during the Paleocene [*Lemarchand et al.*, 2000], as well as low surface ocean pH and thus $B(OH)_4^-$ [*Penman et al.*, 2014; *Anagnostou et al.*, 2016], are thus in qualitative agreement with the lower overall B/Ca ratios of Paleocene foraminifera.

4.2. Effects of PO_4^{3-}

Henehan et al. [2015] recently suggested that in sediment core-top and plankton tow samples, seawater $[PO_4^{3-}]$ may be more closely related to B/Ca than carbonate system parameters. The authors hypothesized that increased $[PO_4^{3-}]$ may cause B/Ca to increase by either promoting amorphous calcium carbonate precipitation, via paired substitution of PO_4^{3-} and $B(OH)_4^-$ ions to maintain charge balance in the crystal, or due to a growth rate effect driven by increased food availability in high-nutrient areas. *Howes et al.* [2017] further suggest that the apparent correlation is driven by increased symbiont photosynthesis under high $[PO_4^{3-}]$, which raises the pH of the foraminiferal microenvironment and thus B/Ca. While we did not

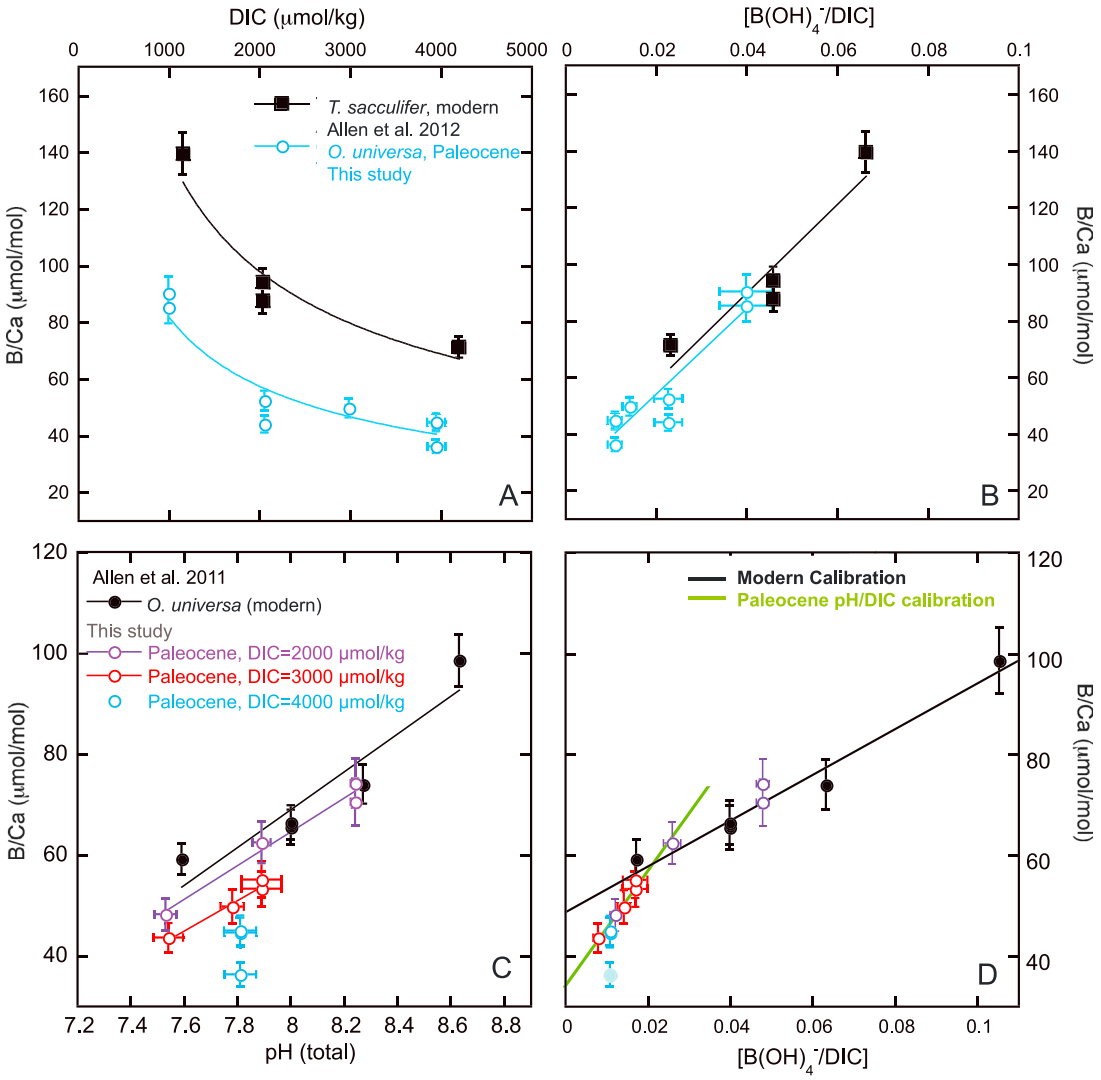

Figure 4. Response of B/Ca to (a and b) variable DIC at constant pH and to (c and d) variable pH at two constant DIC concentrations under simulated Paleocene seawater chemistry. Data from simulated Paleocene experiments (colored symbols) are shown in comparison to experiments conducted under modern seawater conditions (black symbols) [*Allen et al.*, 2011, 2012]. Both pH and DIC force B/Ca along the same calibration slope at low $[B(OH)_4^-]$/DIC (Figure 4, green line), which can be used to estimate the relative influence of pH and DIC on B/Ca during the PETM. In Figure 4d, two replicates from the 4000 μmol kg^{-1} DIC at pH_{Tot} = 7.8 experiment (blue) are included in the pH/DIC calibration. The lower replicate is not included (light blue filled circle, see text for explanation). The error bars are 2σ.

perform specific $[PO_4^{3-}]$ experiments, the nutrient values in our artificial seawater solutions were at 0.5× ambient concentrations as no nutrients were added to our 50% natural, 50% synthetic seawater mixture. The possible effect of low $[PO_4^{3-}]$ can most easily be considered in $[B]_T$ experiments, where a $[PO_4^{3-}]$ effect should cause lower B/Ca compared to the 1.0 and 5.0× $[B]_T$ experiment data of *Allen et al.* [2011]. We do not observe a marked negative offset in B/Ca in these experiments over what is expected from the linear relationship established by *Allen et al.* [2011] where $[PO_4^{3-}]$ was at full seawater values (Figure 3a); instead, all $[B]_T$ experiments fall directly in line with each other. This indirect result suggests that $[PO_4^{3-}]$ is unlikely a major control on B/Ca in our experiments. However, culture experiments deliberately investigating the effects of a wide range of nutrient concentrations on foraminiferal growth, symbiont photosynthesis, and trace element ratios may yield further insight into the controls on B/Ca in natural settings.

4.3. Evaluating Saturation and Average Shell Growth Rate Effects on Foraminiferal B/Ca

Recent inorganic precipitation experiments have found that B/Ca increases with synthetic calcite growth rate [*Mavromatis et al.*, 2015; *Uchikawa et al.*, 2015; *Gabitov et al.*, 2014]. In the study of *Uchikawa et al.* [2015], this conclusion is based on the observation that high-[Ca] and high-DIC conditions lead to elevated B/Ca uptake

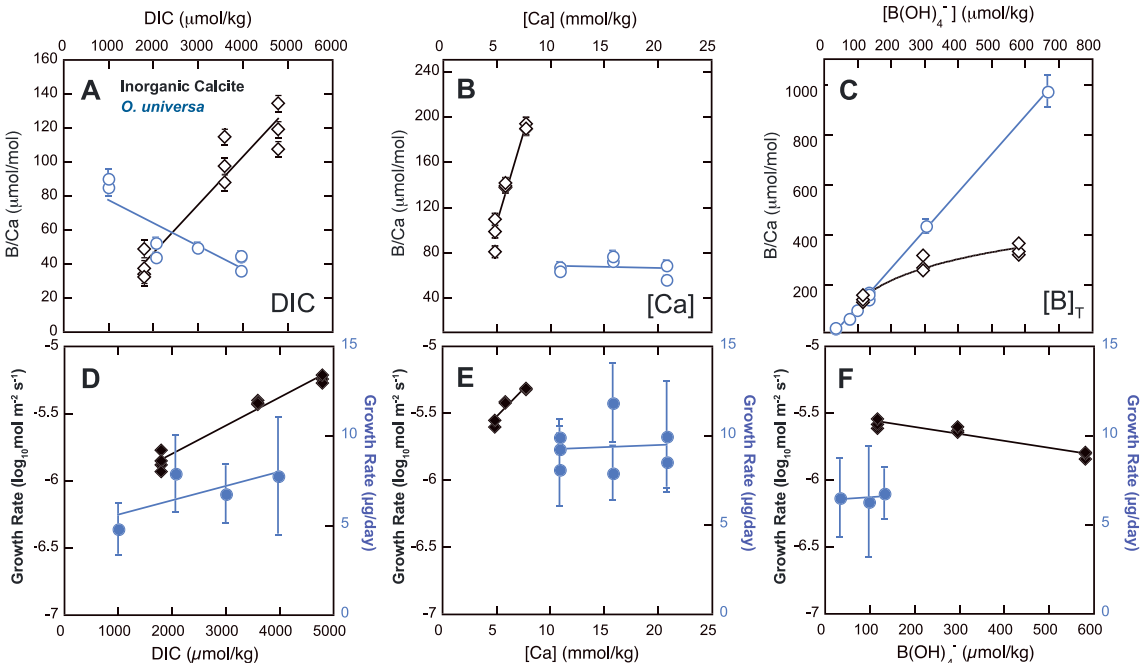

Figure 5. Relationships of (top row) B/Ca and (bottom row) growth rate with experimental parameters in our experiments and in inorganic calcites [*Uchikawa et al.*, 2015]. Growth rate in foraminifers is shown in μg/d (right axis, blue) and are compared against area-normalized rates of *Uchikawa et al.*, 2015 (black diamonds). Note that inorganic calcite rates are expressed on a log scale, and comparison of these values to foraminifer growth rate in μg d^{-1} is only for demonstration of relative trends. In C, data from this study and from *Allen et al.* [2011] are shown (see Figure 3). The error bars on *O. universa* growth rates are 1σ.

into synthetic calcite in the absence of a [$B(OH)_4^-$] increase (Figures 5a and 5b, black diamonds). If the same systematics apply to planktic foraminifera and given that a major reduction in surface ocean $CaCO_3$ saturation likely occurred across the PETM [*Penman et al.*, 2014] and seawater [Ca] was much higher in the past [*Lowenstein et al.*, 2014], the surface ocean acidification signal recorded by planktic foraminiferal B/Ca at the PETM could be compromised by these competing effects.

To investigate trends in foraminiferal growth rate across our experimental parameters, we used shell weight and duration of life data from our experiments to estimate average shell growth rates. These do not reflect instantaneous calcification rates but give an indication of average relative foraminiferal growth in our experiments. We first consider shell weights independently as an indicator for growth rate, without making assumptions about the duration of calcification. Shell weight shows a significant increase with seawater DIC ($p = 0.009$); in experiments ranging from DIC = 1000 to 4000 μmol kg^{-1}, average shell weight more than doubles (28 ± 11 to 67 ± 23 μg 1σ; Figure 2 and Table S2). When growth rates are calculated using the duration of sphere thickening as the time constraint in μg d^{-1}, foraminifers grown in low DIC still have lower growth rates, but the rest of the DIC experiments (2000–4000 μmol kg^{-1}) have similar values and the relationship is no longer statistically significant (Figures 2 and 5). Nevertheless, both parameters indicate that at low DIC, foraminiferal growth rate may be hampered.

If growth rate were the controlling factor on planktic foraminiferal B/Ca, B/Ca should thus decrease at low DIC, as was observed in inorganic calcites [*Uchikawa et al.*, 2015]. However, this is not the case: B/Ca decreases in planktic foraminifera when DIC *increases* (Figure 5a) [*Allen et al.*, 2012, *Howes et al.*, 2017]. Instead, this observation in foraminifera is consistent with competition between $B(OH)_4^-$ and DIC ions during calcification (and thus a [$B(OH)_4^-$]/DIC or [$B(OH)_4^-/HCO_3^-$] control on the proxy), rather than a strong modulation by growth rate [see also, *Allen et al.*, 2016]. In addition, the slopes of the B/Ca response to DIC between both *O. universa* (this study) and *T. sacculifer* [*Allen et al.*, 2012] are nearly indistinguishable (Figure 4b). This may further suggest that the response to DIC is more inorganically driven by the competition of $B(OH)_4^-$ and DIC ions, as average shell growth rate has been found to be greater in cultured *O. universa* compared to *T. sacculifer* [*Allen et al.*, 2016] and would likely impose a species-dependent effect if it was a major determinant of B/Ca.

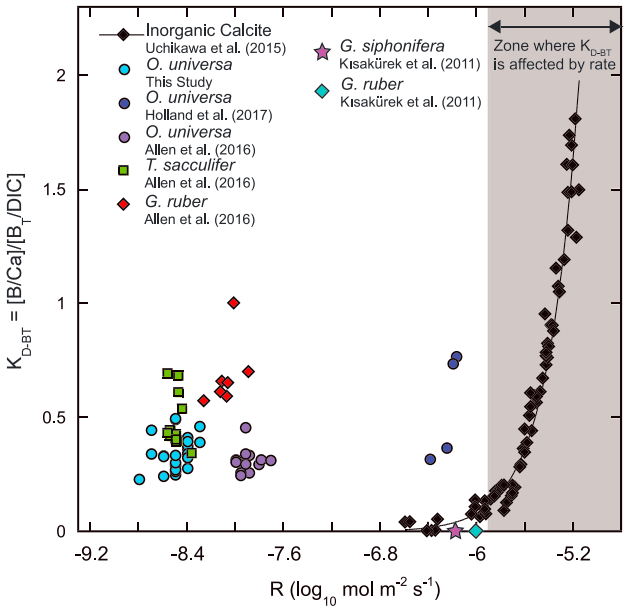

Figure 6. Comparison of estimated foraminiferal and measured inorganic growth rates with the $K_{D\text{-}BT}$ formulation suggested by *Uchikawa et al.* [2015], where B/Ca depends on the $[B]_T$/DIC ratio of seawater. B/Ca was not measured by *Kısakürek et al.* [2011], and growth rates are plotted at zero $K_{D\text{-}BT}$ (purple star and turquoise diamond). Average foraminiferal shell growth rates are lower compared to the range where inorganic calcite $K_{D\text{-}BT}$ and B/Ca are affected by growth rate (grey shaded region).

While shell weights and growth rates in μg d^{-1} are somewhat variable in response to our other experimental parameters ($[B]_T$, [Ca], and pH), they do not show statistical correlation with these parameters at a 90% confidence level (Table S5). Though the large error bars on our growth rate estimates may mask some important variability, the trends between foraminiferal B/Ca itself and these parameters further suggest that growth rate does not control B/Ca in *O. universa* (Figure 5). For example, Uchikawa found that across a narrow range of [Ca] (4–8 mmol/kg), B/Ca nearly doubled (Figure 5b). In contrast, we observe no significant trend in *O. universa* B/Ca when [Ca] was increased from 10 to 20 mmol/kg (p = 0.95; Figures 3b and 5). The lack of a trend in B/Ca with [Ca] confirms a few mechanistic underpinnings of the proxy. First, B does not substitute for Ca^{2+} in the calcite lattice, as B/Ca should otherwise decrease with increasing [Ca]. In addition, Ca-$B(OH)_4^-$ complexes are likely not involved in calcification, which would predict a positive correlation. Finally, the saturation-induced effect on B/Ca observed in inorganic calcites is not borne out in *O. universa*.

A lack of growth rate effect on B/Ca in *O. universa* compared to inorganic calcites may also explain the variable response of B/Ca to $[B]_T$ in the two forms of calcite. *Uchikawa et al.* [2015] found that in $[B]_T$ experiments, high $[B]_T$ may itself inhibit growth rate, which would consequently decrease boron incorporation at high $[B]_T$, explaining the asymptotic increase of B/Ca with $[B]_T$ in calcites (Figures 5c and 5f). In *O. universa*, however, B/Ca continues to increase linearly between 0.5 and 10× $[B]_T$ [*Allen et al.*, 2011; this study]. This offers further evidence that crystal habit and growth rate appear to be under tighter biological control in foraminifera [*Allen et al.*, 2016], as B incorporation does not appear to be retarded by a decline in growth rate.

Allen et al. [2016] suggest that area-normalized foraminiferal growth rates appear to fall below the range where B/Ca in inorganic calcites is strongly affected by rate [*Uchikawa et al.*, 2015]. We also plot our area-normalized growth rate estimates (Table S2) versus *Uchikawa et al.*'s [2015] proposed controlling parameter, K_D = [B/Ca]/[$[B]_T$/DIC]. In agreement with previous studies [*Kısakürek et al.*, 2011; *Holland et al.*, 2017, and *Allen et al.*, 2016], our estimates of area-normalized growth rate using BET surface area measurements of *O. universa* are below the threshold for strong dependence of B/Ca on rate, and in our case by 2 orders of magnitude (Figure 6). Thus, while growth rate may be somewhat variable in planktic foraminifers (Figures 2 and 5) [*Lea et al.*, 1995], these variations are unlikely within the window of growth rates where B/Ca is significantly affected in inorganic precipitates. In the context of Paleocene reconstructions, we suggest that B/Ca records generated over periods of extreme changes in saturation, such as the PETM, can be interpreted in a framework assuming that the $[B(OH)_4^-]$/DIC (or $[B(OH)_4^-/HCO_3^-]$) ratio is the main control on the proxy without significant contribution from saturation-induced growth rate changes or seawater [Ca].

However, our estimates of relatively slow growth rates do not preclude the notion that instantaneous growth rates during calcification could be momentarily faster, for which daily or hourly estimates would be needed to confirm our findings. Multiple authors suggest that foraminiferal calcification rates vary throughout the organism's life cycle and from day to night [*Lea et al.*, 1995; *Spero*, 1988; *Spero et al.*, 2015], and we cannot

rule out that instantaneous rates could be faster than the apparent threshold for B/Ca dependence on rate. This is possible particularly during gametogenic crust deposition, which occurs over a very short period at the end of the foraminifer's life cycle in *O. universa* [*Hamilton et al.*, 2008]. However, without laser ablation or electron microprobe mapping of individual shells, we cannot quantify gametogenic calcite contribution in this study. In addition, our estimates of growth rates in culture are at odds with two recent studies suggesting a rate control on planktic foraminfieral B/Ca from sediment traps [*Salmon et al.*, 2016] and from core-top samples [*Quintana Krupinski et al.*, 2017]. *Quintana Krupinski et al.* [2017] argued indirectly for a rate control, showing that that B/Ca has the strongest correlation with $\Omega_{calcite}$ in their core-top samples of *G. bulloides* and *N. incompta* [*Quintana Krupinski et al.*, 2017]. However, because $\Omega_{calcite}$ also significantly covaries with $[B(OH)_4^-]$/DIC and $[B(OH)_4^-]/[HCO_3^-]$, we thus cannot rule out a $[B(OH)_4^-]$/DIC or a $[B(OH)_4^-]/[HCO_3^-]$ control on B/Ca in their data set. Curiously, the results of *Salmon et al.* [2016], who used test area density as a proxy for shell thickness (in $\mu g/\mu m^2$ calcite) and thus growth rate, directly conflict with the culture results of *Allen et al.* [2016], who estimated average growth rates in $\mu g\ d^{-1}$. *Salmon et al.* [2016] found that test area density was higher in *G. ruber* compared to *O. universa*, while *Allen et al.* [2016] found the opposite trend. Given the strong relationship between growth rate and B/Ca in inorganic calcites and these divergent results between natural and cultured foraminifera samples, we suggest that instantaneous foraminiferal growth rates should be better studied in culture with geochemical tracers. Further analysis of intrashell trace element trends coupled with growth rate monitoring will help to illuminate these controls at the microscale.

4.4. Light and Size Effects on B/Ca in *Orbulina universa*

Given that multiple studies have found that low-light conditions caused reduced symbiont photosynthesis and thus a reduction in pH near the foraminiferal calcifying environment [*Rink et al.*, 1998; *Köhler-Rink and Kühl*, 2005], we might expect that low-light conditions would cause a decline in B/Ca. Contrary to prediction, we do not find lower B/Ca ratios in our low-light experiment from Santa Catalina Island, where light levels were significantly below light saturation for photosynthesis (19 μmol photons/m^2/s; Figure 3c). However, we do observe a pronounced decrease in B/Ca in low-light experiments from Puerto Rico (PR, from 70 to 58 μmol/mol). The spectral quality of light used between the two culture seasons was exactly the same, and so this cannot explain the differences we observe between the two sites (see section 2). Previously unpublished culture experiments do suggest a higher sensitivity of *O. universa* B/Ca to pH in PR compared to Catalina (Figure S1), which could make the effect more pronounced in PR experiments. Based on the 1.5‰ $\delta^{11}B$ difference between *O. universa* grown in high-light and low-light experiments observed by *Hönisch et al.* [2003], the integrated pH signal recorded by low-light *O. universa* shells has been quantified at −0.2 units compared to ambient conditions. Based on this estimate, the Catalina B/Ca versus pH calibration of *Allen et al.* [2011] predicts that low-light B/Ca should be ~7 μmol/mol lower, while the more sensitive B/Ca calibration from PR predicts a decrease of 11 μmol/mol. Given that 2σ uncertainty for ambient B/Ca ~65 μmol/mol is ±4 μmol/mol (±6.6%), the predicted light effect of −7 μmol/mol on Catalina may thus be too small to be detectable.

In addition, *O. universa* from PR could have a more sensitive microenvironment pH response to low light than those from Catalina Island. One possibility is that this variable response is related to genetic differences between regional populations of *O. universa*. *Darling and Wade* [2008] showed that a different genotype of *O. universa* is present in the Caribbean (Type I) versus Southern California (Type III). If the genetic differences are expressed in physiological differences, such as differences in symbiont density, other pH-sensitive ions should change in PR low-light experiments and not in Catalina experiments. For instance, shell Mg/Ca has been observed to increase at lower than ambient seawater-pH [*Lea et al.*, 1999, *Russell et al.*, 2004, *Evans et al.*, 2016] and should thus increase under low-light conditions. Indeed, average Mg/Ca increases by 0.91 mmol/mol (10%) in PR low-light experiments and does not change in Catalina experiments (Figure 7a). This observation supports the notion that *O. universa* from the two study sites may show a significantly different microenvironment response to low light intensity.

Overall, our results tentatively support the hypothesis put forth by *Babila et al.* [2014] that light intensity can have a small effect on B/Ca in planktic foraminifera, although different genotypes of the same morphospecies appear to display differences in sensitivity. If foraminifers did fully "bleach" at the PETM, it is conceivable that this could have a small effect on B/Ca records. However, analyses of $\delta^{11}B$ and $\delta^{13}C$ of different size

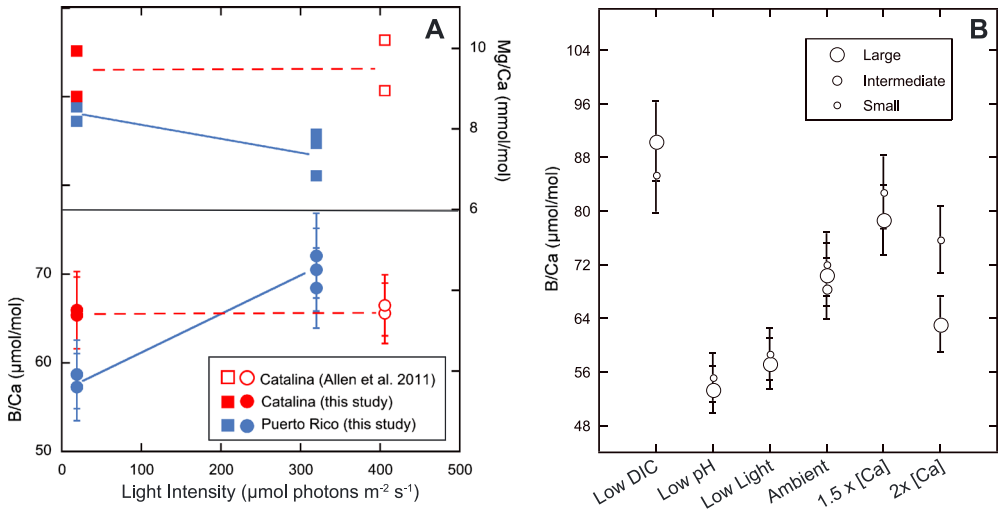

Figure 7. Effects of test size and low-light conditions on B/Ca and Mg/Ca in select experiments. (a) Mg/Ca (top, squares) and B/Ca (bottom, circles) from low-light experiments from Puerto Rico (blue) and Santa Catalina Island (red) are shown. (b) Relative size fractions for each experiment are shown in large, intermediate, and small circles (Table S2). Size fraction replicates are almost always within analytical uncertainty (2σ).

fractions of symbiont-bearing species across the PETM do not provide any evidence for a reduction of the symbiont association [*Penman et al.*, 2014; *Babila et al.*, 2016], arguing against a significant "bleaching" effect. Careful analysis of isotopic trends with size is advisable however to constrain this effect in future studies.

We also investigate whether shell size has a significant effect on B/Ca in *O. universa*. Increased B/Ca in larger specimens of *G. ruber* and *T. sacculifer* from sediment traps has been hypothesized to result from increased growth rates in larger individuals [*Ni et al.*, 2007]. Except for the 2× [Ca] experiment, our size fraction replicates do not suggest a size fraction effect on B/Ca. At 2× [Ca], large individuals (607–664 µm) have significantly lower B/Ca than smaller ones (528–598 µm; Figure 7b). Because our simulated Paleocene experiments were also conducted at 20 mmol/kg [Ca], it is not clear why these conditions alone should cause a significant size fraction effect. Regardless of the results from this one experiment, shell size alone does not appear to systematically influence B/Ca in *O. universa*. This suggests that any variability in growth rate between size fractions of *O. universa* is not large enough to affect B/Ca. However, B/Ca has been found to increase with size in sediment core samples of *T. sacculifer* and *G. ruber* [*Ni et al.*, 2007] and sediment trap samples in *G. ruber* [*Babila et al.*, 2014], warranting further investigation of size effects in culture in these species.

4.5. Carbonate Chemistry Experiments

In order to more accurately constrain surface ocean carbonate chemistry shifts across the PETM, we conducted a matrix of experiments to investigate how B/Ca responds to both pH and DIC under constant simulated Paleocene seawater chemistry. Given our consistent results in [Ca], DIC, and $[B]_T$ experiments, we assume that the $[B(OH)_4^-]$/DIC ratio of seawater is the controlling parameter on B/Ca [*Allen et al.*, 2012] without a major growth rate influence. As indicated above, both $[B(OH)_4^-]$/DIC and $[B(OH)_4^-/HCO_3^-]$ are viable control parameters, but the practical difference between them is minimal, and we therefore adopt the $[B(OH)_4^-]$/DIC calibration for the sake of simplicity.

Using the York Fit method in MATLAB, we report linear calibrations for B/Ca versus DIC, B/Ca versus pH at constant DIC = 2000 µmol kg^{-1}, and B/Ca versus pH at constant DIC = 3000 µmol kg^{-1} (Table 2). Both of our Paleocene pH calibrations show markedly different behavior at low seawater $[B(OH)_4^-]$/DIC, which is a probable background condition of the Paleocene surface ocean, considering that it was likely characterized by low pH [*Penman et al.*, 2014; *Anagnostou et al.*, 2016] and low $[B]_T$ [*Lemarchand et al.*, 2000]. When pH_{Tot} decreases from 7.9 to 7.5 at a constant DIC of 2000 µmol kg^{-1}, B/Ca decreases significantly below the modern

Table 2. Calibration Equation Coefficients and Calculated Intercepts Shifted Through Pre-PETM Conditions

Calibration	Slope	95% C.I.	Intercept	95% C.I.	Shifted Intercept	Predicted Peak-PETM $[B(OH)_4^-]/DIC$
DIC, Constant pH	1553	251	24.0	3.8	20.4	0.0155
pH, DIC = 2000 μmol/kg	664	133	41.6	4.3	49.0	−0.0068
pH, DIC = 3000 μmol/kg	1137	489	34.4	6.6	33.8	0.0094
Combined pH/DIC[a]	1147	284	33.7	4.0	33.5	0.0096
Allen et al. [2011]	425	67	50.1	3.3	56.7	−0.0287

[a]The "Paleocene" calibration where $[B(OH)_4^-]/DIC < 0.03$.

calibration, suggesting higher calibration sensitivity (Figure 4d, purple circles). This same increase in sensitivity with the same apparent slope is also seen in pH experiments at constant DIC of 3000 μmol kg^{-1}, which all fall below $[B(OH)_4^-]/DIC = 0.03$ (Figure 4d, red circles). In addition, B/Ca data from both sets of pH experiments (at constant DIC = 2000 μmol kg^{-1} and constant DIC = 3000 μmol kg^{-1}) converge to one calibration line below a $[B(OH)_4^-]/DIC$ ratio of 0.03 (Figure 4d). This implies that the response of B/Ca to $[B(OH)_4^-]/DIC$ by decreasing pH or by increasing DIC has the same, more sensitive, calibration slope below $[B(OH)_4^-]/DIC = 0.03$. It should be noted that this is not an artifact of using $[B(OH)_4^-]/DIC$ as the controlling parameter, as the result is the same when $[B(OH)_4^-/HCO_3^-]$ is used (Figure S3).

Given the convergent sensitivity of B/Ca to $[B(OH)_4^-]/DIC$ in both pH and DIC experiments at these low values, it follows that other data from our DIC experimental matrix at constant pH = 7.8 (i.e., DIC = 4000 and 2050 μmol kg^{-1}) should fall along the same line. However, data from the DIC = 2050 μmol kg^{-1} experiment do not have good reproducibility; they fall below the line and are also lower than anticipated from the regression of the other DIC experiments (Figure 4b). Mn/Ca ratios in the experimental seawater and the corresponding foraminifera shells were 2 orders of magnitude higher in this experiment than in any other, which indicates some form of contamination, and we thus do not include these data in our analysis (Figure S6). Data from the 4000 μmol kg^{-1} DIC experiment do fall onto the calibration, with good reproducibility for two out of three replicates (Table 1 and Figure 4b). When the one low replicate data point is included in the calibration, this greatly increases the calibration sensitivity (see Text S6). This replicate does not show any evidence for contamination, but based on sample weights was primarily composed of calcite from two large individuals, which may not have been representative of the entire shell population. Though this would allow us to explain a greater proportion of the B/Ca excursion, it would be spurious to hinge our interpretation on this one replicate. To err on the side of caution, we therefore define a combined calibration for B/Ca versus both pH and DIC at low $[B(OH)_4^-]/DIC$ up to a DIC of 4000 μmol kg^{-1} (<0.03 $[B(OH)_4^-]/DIC$; Figure 4d, green line, and Table 2) but exclude the low replicate in our analysis here.

What can explain the increased sensitivity of B/Ca to $[B(OH)_4^-]/DIC$ in our simulated Paleocene acidification experiments? *Allen et al.* [2011] showed that in *O. universa*, B/Ca has lower sensitivity to changing $[B(OH)_4^-]$ when pH is increased compared to when $[B]_T$ is increased (see their Figure 2). We argue that this suggests that *O. universa* is able to buffer large swings in pH near the calcifying microenvironment, possibly by cellular pH regulation. Multiple authors have suggested that foraminifers increase their cellular pH to promote calcification [e.g., *Toyofuku et al.*, 2017; *de Nooijer et al.*, 2009]. This mechanism would be particularly necessary at low ambient pH, where *Evans et al.* [2016] note that foraminifers may need to "try harder" to raise intracellular pH. Given that in our Paleocene pH calibration, B/Ca is lower than expected from the modern pH calibration, a pH regulation mechanism may not be as active under the low Mg/Ca_{sw} conditions in our experiments (i.e., Mg/Ca_{sw} = 1.5 mol/mol, compared to a ratio of 5.1 mol/mol in the modern ocean). *Zeebe and Sanyal* [2002] found that removal of Mg from seawater allows inorganic calcites to precipitate at much lower pH levels (8.2 instead of 9.9, on the NBS scale). It follows that at low Mg/Ca_{sw}, foraminifers may not need to raise the pH of the calcifying microenvironment as much to promote calcification, causing B/Ca to be relatively diminished at low $[B(OH)_4^-]/DIC$ under low Mg/Ca_{sw} and thus showing increased calibration sensitivity. In this model, at ambient pH, requirements for cellular pH modification would be lower, causing the calibrations to converge when $[B(OH)_4^-]/DIC > 0.03$. Culture experiments at low pH with variable Mg/Ca could test this hypothesis.

It is also possible that the relationship of B/Ca with $[B(OH)_4^-]$/DIC becomes nonlinear at low $[B(OH)_4^-]$/DIC and is better suited by one logarithmic regression rather than two linear ones (Figure S6). This implies that foraminifers grown under modern seawater chemistry may show the same nonlinear behavior if they were cultured at these low $[B(OH)_4^-]$/DIC values. To address this, more experiments at low $[B(OH)_4^-]$/DIC and otherwise modern seawater chemistry are warranted. However, there is clear divergence in the behavior of pH and DIC experiments when $[B(OH)_4^-]$/DIC > 0.03, as B/Ca in the low DIC experiment (1000 μmol kg^{-1}) is much higher than the pH experiments at a similar $[B(OH)_4^-]$/DIC (Figure S6). This indicates that a single logarithmic regression does not satisfactorily describe the relationship between B/Ca and $[B(OH)_4^-]$/DIC. Given the convergent behavior at low values in our experiments, and that the Paleocene ocean likely had low $[B(OH)_4^-]$/DIC [*Penman et al.*, 2014], we therefore adopt our linear calibration with increased sensitivity for application to this time period.

4.6. Application of New Calibrations

First principles suggest that during the PETM, pH should have decreased and total DIC increased due to the combined effects of CO_2 injection, seafloor $CaCO_3$ dissolution, and on >100 kyr timescales, increased riverine input by enhanced continental weathering [*Zeebe et al.*, 2009, *Komar and Zeebe*, 2011, *Penman*, 2016]. Our Paleocene calibrations now allow us to combine published δ^{11}B-derived pH estimates [*Penman et al.*, 2014] with various scenarios for DIC change to evaluate the conditions necessary to explain the observed B/Ca excursion [*Penman et al.*, 2014]. As a first step, we investigate the peak-PETM $[B(OH)_4^-]$/DIC ratios that are predicted for each of our calibrations, given the magnitude of the B/Ca excursion of *Penman et al.* [2014]. While previous *O. universa* calibrations predicted negative $[B(OH)_4^-]$/DIC ratios, our Paleocene calibrations yield more reasonable peak-PETM $[B(OH)_4^-]$/DIC ratios when applied to *M. velascoensis* B/Ca data (Table 2). Our Paleocene calibration for pH at DIC = 2000 μmol kg^{-1} still predicts a negative $[B(OH)_4^-]$/DIC ratio (−0.007), which is largely driven by the $pH_{Tot} = 8.3$ data point. However, peak-PETM $[B(OH)_4^-]$/DIC becomes positive in our combined calibration for pH and DIC when $[B(OH)_4^-]$/DIC < 0.03 and in our DIC = 3000 μmol kg^{-1} pH calibration (Table 2). This further supports that the increased sensitivity we observe at low seawater $[B(OH)_4^-]$/DIC is more applicable to PETM data and that increased DIC amplifies the PETM B/Ca excursion given increased sensitivity at low $[B(OH)_4^-]$/DIC.

As a next step, we predict the B/Ca excursion resulting from the δ^{11}B-derived surface ocean pH decrease using both the "Modern" calibration of *Allen et al.* [2011] and our new Paleocene calibration for both pH and DIC at $[B(OH)_4^-]$/DIC <0.03. For the initial calculation we hold DIC constant at 2000 μmol kg^{-1} and only consider the $[B(OH)_4^-]$ decrease in response to the pH decrease inferred from δ^{11}B [*Penman et al.*, 2014]. The resulting Paleocene B/Ca excursion (Figure 8b) is larger than what is predicted by the modern seawater calibration (Figure 8a) but is still smaller than measured by *Penman et al.* [2014] (at a 95% confidence level). We can now take the next step and calculate the pulse of DIC that is necessary to explain the full peak-PETM B/Ca excursion, but to do so, we have to extrapolate our combined pH/DIC calibration to the PETM B/Ca ratio of 44.5 μmol/mol, which implies higher DIC values than simulated in our experiments (>4000 μmol kg^{-1}). The calculated DIC from this exercise is shown in Figure 8c and displays an extraordinarily large DIC pulse from the background level of 2000 μmol kg^{-1} to ~4500 μmol kg^{-1} on average immediately at the PETM. In comparison, the model estimates of *Zeebe et al.* [2009] suggest a slow increase on the order of ~350 μmol kg^{-1} DIC in the Pacific surface ocean (Figure 8c), indicating that the carbonate chemistry shift predicted by the B/Ca proxy is significantly larger than conceived by the model. This discrepancy is similar to the larger pH excursion inferred from δ^{11}B (i.e., ~ −0.3 units [*Penman et al.*, 2014]) compared to the −0.18 units from a LOSCAR model run, though *Penman et al.* [2014] suggested that increasing the strength of organic carbon remineralization [*Matsumoto*, 2007] in the model parameterization brings δ^{11}B and modeled pH excursions more into line.

It is additionally possible that other contributing factors have amplified the B/Ca excursion recorded at the PETM, such as loss of B during peak acidification or postdepositional diagenesis. *Penman et al.* [2014] discuss the possible effects of sediment dissolution on their trace element records and conclude soundly that dissolution cannot account for the entire B/Ca excursion. This is because a pronounced Mg/Ca excursion is also recorded and because B/Ca remains low long after sediment dissolution recovered. Recently, however, *Edgar et al.* [2015] showed that diagenetic alteration caused B loss from Eocene planktic foraminifers

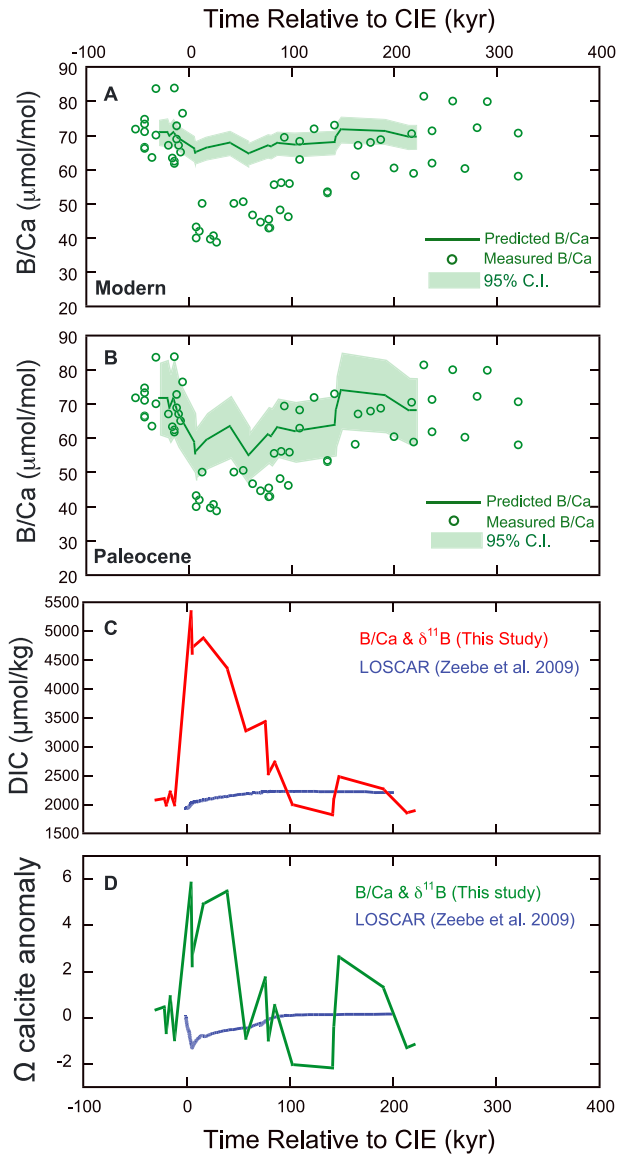

Figure 8. Translation of published PETM *M. velascoensis* B/Ca data from ODP site 1209 to surface ocean carbonate chemistry. (a and b) The *O. universa* B/Ca shift in response to surface ocean acidification (using $\delta^{11}B$ data of *Penman et al.* [2014]; solid green lines], using the modern *O. universa* pH calibration (Figure 8a) [*Allen et al.*, 2011] and our Paleocene calibration (Figure 8b). The shaded green areas show the 95% confidence interval of the predicted excursion. The open symbols reflect actual measured B/Ca ratios [*Penman et al.*, 2014]. (c) We use our combined pH and DIC relationship to calculate the DIC increase needed to explain the remainder of the B/Ca excursion, showing a DIC pulse of up to ~2500 μmol kg^{-1} compared to the small increase predicted by LOSCAR for the surface Pacific Ocean [*Zeebe et al.*, 2009, blue line]. (d) The corresponding Ω anomaly of the two cases.

displaying frosty preservation, in comparison to contemporaneous glassy specimens. *Babila et al.* [2016] measured B/Ca from a shallow marine section spanning the PETM off the New Jersey Margin, in which glassy foraminifers were used for analysis. The authors note that the magnitude of the B/Ca excursion is very similar to the excursion observed at Site 1209, suggesting instead that diagenetic overprinting at the open ocean site is not a major contributor to the B/Ca signal, lending confidence to the size of the excursion recorded at Site 1209. Nevertheless, diagenetic alteration still imposes a potential bias on these trace element records that span a time of extreme undersaturation. However, lacking evidence to the contrary, we proceed assuming that the consistent results from the two disparate sites support the large amplitude of the B/Ca excursion at Site 1209.

We further test the feasibility of our DIC estimates by using reconstructed pH (from $\delta^{11}B$) and DIC (from B/Ca) to calculate the corresponding surface ocean calcite saturation state Ω in CO2sys.m (see section S6). Whereas the size of the DIC excursion predicted by models such as LOSCAR is likely also affected by model parameterization, the result from our reconstruction is ultimately untenable, as the inferred pH and DIC excursions imply an increase in surface ocean $\Omega_{calcite}$ from 8 to ~12 (Figure 8d and Table S6). This is inconsistent with evidence of widespread seafloor dissolution as well as modeled surface ocean Ω estimates that predict a decrease in surface ocean saturation at the PETM [*Zachos et al.*, 2005, *Penman et al.*, 2014] (Figure 8d). Consequently, although our Paleocene *O. universa* calibration yields positive, and therefore more reasonable $[B(OH)_4^-]$/DIC values, it still appears too insensitive to satisfactorily explain the B/Ca shift measured in *M. velascoensis* across the PETM. In addition, including the lower DIC replicate in the calibration (see section 4.5, section S6, and Figure S7) drastically reduces the predicted DIC estimate and predicts no consistent change in Ω across the PETM, implying that uncertainties on this calculation at this time are too large for quantitative application. We therefore also refrain from estimating pCO_2 at this time, as such a

reconstruction would be fraught with uncertainty. However, the B/Ca sensitivity to pH in *O. universa* is much less than that observed in *G. ruber* and *T. sacculifer* [*Allen et al.*, 2012] (Figure S1), and B/Ca systematics in *O. universa* alone may thus not be appropriate for Paleocene foraminifera species. Investigating the response of B/Ca in other symbiont-bearing planktic foraminifera to pH and low $[B(OH)_4^-]$/DIC under Paleocene seawater conditions will add more certainty to carbonate chemistry estimates for the PETM.

5. Conclusions

In *O. universa*, the B/Ca response to pH, DIC, and $[B]_T$ under simulated Paleocene seawater conditions parallels results from previous culture studies in modern seawater composition [*Allen et al.*, 2011; *Allen et al.*, 2012] and confirms that B/Ca increases with pH and $[B]_T$ but is inversely correlated with DIC. B/Ca in *O. universa* does not show any increase with [Ca], suggesting that the growth rate effect observed in inorganic precipitates does not apply to this foraminifera species. Our estimates of average foraminifer shell growth rates, along with the B/Ca response to varying DIC, [Ca], and $[B]_T$, instead support the previously postulated $[B(OH)_4^-]$/DIC or $[B(OH)_4^-]/[HCO_3^-]$ control on the proxy. Low-light conditions cause a decrease in B/Ca in *O. universa* from Puerto Rico but not from Santa Catalina Island, suggesting a differential physiological sensitivity between subpopulations of the same species. Shell size does not consistently modify B/Ca within measurement uncertainty in this species. Pairing low pH with high-DIC conditions, the sensitivity of the B/Ca proxy increases in simulated Paleocene seawater chemistry. This improves carbonate and borate chemistry estimates for the PETM compared to calibrations with *O. universa* grown in modern seawater. However, estimates of the DIC input at the PETM, calculated from our new calibrations coupled with $\delta^{11}B$-derived pH estimates, are untenably large and inconsistent with observations of carbonate dissolution at the seafloor at that time. Further calibrations with other foraminifera species and confirmation of the paleo-surface ocean B/Ca shift from additional locations will be critical in further constraining carbonate chemistry changes across the PETM.

Acknowledgments
We thank Jordan Snyder, Alex Gagnon, Sam Phelps, Jennifer Fehrenbacher, Catherine Davis, and Ann Russell, who assisted in the collection of foraminifers, and Caroline Baptist and Nina Ruprecht for their laboratory assistance. Stella Woodard, Ryan Bu, and Paola Moffa-Sanchez provided assistance with ICP-MS analyses at Rutgers. We thank Richard Zeebe for access to LOSCAR model output. Special thanks to Bill Rosado, Govind Nadathur, and Orlando Espinosa for assistance in the lab and on the boat in Puerto Rico. We also thank Kat Allen, Jesse Farmer, Don Penman, and Sidney Hemming for their helpful discussion of the data. This manuscript was greatly improved by the constructive comments of Howie Spero, Michael Henehan, and one anonymous reviewer. This research is funded by NSF [OCE12-32987] to B.H. All data presented in this manuscript can be found in the main text and the supporting information.

References

Allen, K. A., B. Hönisch, S. E. Eggins, L. L. Haynes, Y. Rosenthal, and J. Yu (2016), Trace element proxies for surface ocean conditions: A synthesis of culture calibrations with planktic foraminifera, *Geochim. Cosmochim. Acta*, *193*, 197–221, doi:10.1016/j.gca.2016.08.015.

Allen, K. A., and B. Hönisch (2012), The planktic foraminiferal B/Ca proxy for seawater carbonate chemistry : A critical evaluation, *Earth Planet. Sci. Lett.*, *348*, 203–211, doi:10.1016/j.epsl.2012.06.012.

Allen, K. A., B. Honisch, S. M. Eggins, and Y. Rosenthal (2012), Environmental controls on B/Ca in calcite tests of the tropical planktic foraminifer species *Globigerinoides ruber* and *Globigerinoides sacculifer*, *Earth Planet. Sci. Lett.*, *351*, 270–280, doi:10.1016/j.epsl.2012.07.004.

Allen, K. A., B. Hönisch, S. M. Eggins, J. Yu, H. J. Spero, and H. Elderfield (2011), Controls on boron incorporation in cultured tests of the planktic foraminifer *Orbulina universa*, *Earth Planet. Sci. Lett.*, *309*(3–4), 291–301, doi:10.1016/j.epsl.2011.07.010.

Al-Ammar, A. S., R. K. Gupta, and R. M. Barnes (2000), Elimination of boron memory effect in inductively coupled plasma-mass spectrometry by ammonia gas injetion into the spray chamber during analysis, *Spectrochim. Acta, Part B*, *55*(6), 629–635, doi:10.1016/S0584-8547(00)00197-X.

Anagnostou, E., E. H. John, K. M. Edgar, G. L. Foster, A. Ridgwell, G. N. Inglis, R. D. Pancost, D. J. Lunt, and P. N. Pearson (2016), Changing atmospheric CO_2 concentration was the primary driver of early Cenozoic climate, *Nature*, *533*, 380–384, doi:10.1038/nature17423.

Babila, T. L., Y. Rosenthal, and M. H. Conte (2014), Evaluation of the biogeochemical controls on B/Ca of *Globigerinoides ruber* white from the oceanic flux program, Bermuda, *Earth Planet. Sci. Lett.*, *404*, 67–76, doi:10.1016/j.epsl.2014.05.053.

Babila, T. L., Y. Rosenthal, J. D. Wright, and K. G. Miller (2016), A continental shelf perspective of ocean acidification and temperature evolution during the Paleocene-Eocene Thermal Maximum, *Geology*, *44*(4), 275–278, doi:10.1130/G37522.1.

Brunauer, S., P. H. Emmett, and E. Teller (1938), Adsorption of gases in multimolecular layers, *J. Am. Chem. Soc.*, *60*, 309–319.

D'Hondt, S. D., J. C. Zachos, G. Schultz, and N. Summer (1994), Stable isotopic signals and photosymbiosis in late Paleocene planktic foraminifera, *Paleobiology*, *20*(3), 391–406, doi:10.1017/S0094837300012847.

Darling, K. F., and C. M. Wade (2008), The genetic diversity of planktic foraminifera and the global distribution of ribosomal RNA genotypes, *Mar. Micropal.*, *67*(3–4), 216–238, doi:10.1016/j.marmicro.2008.01.009.

de Kanel, J., and J. W. Morse (1979), A simple technique for surface area determination, *J. Phys. E: Sci. Instrum.*, *12*, 272–273, doi:10.1088/0022-3735/12/4/011.

de Nooijer, L. J., T. Toyofuku, and H. Kitazoto (2009), Foraminifera promote calcification by elevating their intracellular pH, *Proc. Natl. Acad. Sci. U.S.A.*, *106*(36), 15,374–115378, doi:10.1073/pnas.0904306106.

Edgar, K. M., E. Anagnostou, P. N. Pearson, and G. L. Foster (2015), Assessing the impact of diagenesis on d11b, $d^{13}C$, $d^{18}O$, Sr/Ca, and B/Ca values in fossil planktic foraminiferal calcite, *Geochim. Cosmochim. Acta*, *166*, 189–209, doi:10.1016/j.gca.2015.06.018.

Edgar, K. M., S. M. Bohaty, S. J. Gibbs, P. F. Sexton, R. D. Norris, and P. A. Wilson (2013), Symbiont "bleaching" in planktic foraminifera during the Middle Eocene Climatic Optimum, *Geology*, *41*(1), 15–18, doi:10.1130/G33388.1.

Evans, D., B. S. Wade, M. Henehan, J. Erez, and W. Müller (2016), Revisiting carbonate chemistry controls on planktic foraminifera Mg/Ca: Implications for sea surface temperature and hydrology shifts over the Paleocene–Eocene Thermal Maximum and Eocene–Oligocene transition, *Clim. Past Discuss.*, *11*(4), 3143–3185, doi:10.5194/cpd-11-3143-2015.

Foster, G. L. (2008), Seawater pH, pCO_2, and $[CO_3^{2-}]$ variations in the Caribbean Sea over the last 130 kyr: A boron isotope and B/Ca study of planktic foraminifera, *Earth Planet. Sci. Lett.*, *271*, 254–266, doi:10.1016/j.epsl.2008.04.015.

Gabitov, R. I., C. Rollion-Bard, A. Tripati, and A. Sadekov (2014), In situ study of boron partitioning between calcite and fluid at different crystal growth rates, *Geochim. Cosmochim. Acta*, *137*, 81–92, doi:10.1016/j.gca.2014.04.014.

Gehlen, M., F. C. Bassinot, L. Chou, and D. McCorkle (2005), Reassessing the dissolution of marine carbonates: I. Solubility, *Deep Sea Res., Part I*, *52*(8), 1445–1460, doi:10.1016/j.dsr.2005.03.010.

Hain, M. P., D. M. Sigman, J. A. Higgins, and G. H. Haug (2015), The effects of secular calcium and magnesium concentration changes on the thermodynamics of seawater acid/base chemistry: Implications for Eocene and Cretaceous ocean carbon chemistry and buffering, *Global Biogeochem. Cycles*, *29*, 517–533, doi:10.1002/2014GB004986.

Hamilton, C. P., H. J. Spero, J. Bijma, and D. W. Lea (2008), Geochemical investigation of gametogenic calcite addition in the planktonic foraminifera *Orbulina universa*, *Mar. Micropaleontol.*, *68*, 256–267, doi:10.1016/j.marmicro.2008.04.003.

Hemming, N. G., and G. N. Hanson (1992), Boron isotopic composition and concentration in modern marine carbonates, *Geochim. Cosmochim. Acta*, *56*, 537–543, doi:10.1016/0016-7037(92)90151-8.

Henehan, M. J., G. L. Foster, J. W. B. Rae, K. C. Prentice, J. Erez, H. C. Bostock, B. J. Marshall, and P. A. Wilson (2015), Evaluating the utility of B/Ca ratios in planktic foraminifera as a proxy for the carbonate system: A case study of *Globigerinoides ruber*, *Geochem. Geophys. Geosyst.*, *16*, 1052–1069, doi:10.1002/2014GC005514.

Hershey, J. P., M. Fernandez, P. J. Milne, and F. J. Millero (1986), The ionization of boric acid in NaCl, Na-Ca-Cl, and Na-Mg-Cl solutions at 25°C, *Geochim. Cosmochim. Acta*, *50*(1), 143–148, doi:10.1016/0016-7037(86)90059-1.

Holland, K., S. E. Eggins, B. Hönisch, and L. L. Haynes (2017), Calcification rate and microenvironment response of the planktic foraminifer *Orbulina universa* to changing seawater carbonate chemistry, *Earth Planet. Sci. Lett.*, *464*, 124–134.

Hönisch, B., J. Bijma, A. D. Russell, H. J. Spero, M. R. Palmer, R. E. Zeebe, and A. Eisenhauer (2003), The influence of symbiont photosynthesis on the boron isotopic composition of foraminifera shells, *Mar. Micropaleontol.*, *928*, 1–10, doi:10.1016/S0377-8398(03)00030-6.

Howes, E. L., K. Kaczmarek, M. Raitzsch, A. Mewes, N. Bijma, I. Horn, S. Misra, J.-P. Gattuso, and J. Bijma (2017), Decoupled carbonate chemistry controls on the incorporation of boron into *Orbulina universa*, *Biogeosciences*, *14*, 415–430, doi:10.5194/bg-14-415-2017.

Kelly, D. C., T. J. Bralower, and J. C. Zachos (2001), On the demise of the early Paleogene Morozovella velascoensis lineage: Terminal progenesis in the planktonic foraminifera, *Palaios*, *16*(5), 507–523, doi:10.2307/3515565.

Kısakürek, B., A. Eisenhauer, F. Böhm, E. C. Hathorne, and J. Erez (2011), Controls on calcium isotope fractionation in cultured planktic foraminifera, *Globigerinoides ruber* and Globigerinella siphonifera, *Geochim. Cosmochim. Acta*, *75*(2), 427–443, doi:10.1016/j.gca.2010.10.015.

Köhler-Rink, S., and M. Kühl (2005), The chemical microenvironmentl of the symbiotic planktonic foraminifer *Orbulina universa*, *Marine Biol. Res.*, *1*, 68–78, doi:10.1080/17451000510019015.

Komar, N., and R. E. Zeebe (2011), Oceanic calcium changes from enhanced weathering during the Paleocene-Eocene thermal maximum: No effect on calcium-based proxies, *Paleoceanography*, *26*, 1–13, doi:10.1029/2010PA001979.

Lea, D., P. A. Martin, D. A. Chan, H. J. Spero, and H. D. Holland (1995), Calcium uptake and calcification rate in the planktonic foraminifer *Orbulina universa*, *J. Foram. Res.*, *25*(1), 14–23.

Lea, D. W., T. A. Mashiotta, and H. J. Spero (1999), Controls on magnesium and strontium uptake in planktonic foraminifera determined by live culturing, *Geochim. Cosmochim. Acta*, *63*(16), 2369–2379, doi:10.1016/S0016-7037(99)00197-0.

Lee, K., T.-W. Kim, R. H. Byrne, F. J. Millero, R. A. Feely, and Y.-M. Liu (2010), The universal ratio of boron to chlorinity for the North Pacific and North Atlantic oceans, *Geochim. Cosmochim. Acta*, *74*(6), 1801–1811, doi:10.1016/j.gca.2009.12.027.

Lemarchand, D., J. Gaillardet, E. Lewin, and C. J. Allegre (2000), The influence of rivers on marine boron isotopes and implications for reconstructing past ocean pH, *Nature*, *408*, 951–954, doi:10.1038/35050058.

Lowenstein, T. K., B. Kendall, and A. D. Anbar (2014), The geologic history of seawater, in *The Oceans and Marine Geochemistry. Treatise on Geochemistry*, 2nd ed., vol. 8, edited by H. D. Holland and K. K. Turekian, pp. 569–622, Elsevier.

Matsumoto, K. (2007), Biology-mediated temperature control on atmospheric pCO2 and ocean biogeochemistry, *Geophys. Res. Lett.*, *34*, L20605, doi:10.1029/2007GL031301.

Mavromatis, V., B. Montouillout, J. Noireaux, J. Gaillardet, and J. Schott (2015), Characterization of boron incorporation and speciation in calcite and aragonite from co-precipitation experiments under controlled pH, temperature and precipitation rate, *Geochim. Cosmochim. Acta*, *150*, 299–313, doi:10.1016/j.gca.2014.10.024.

Mucci, A., and J. W. Morse (1984), The solubility of calcite in seawater solutions of various magnesium concentration, It = 0.697 m at 25 °C and one atmosphere total pressure, *Geochim. Cosmochim. Acta*, *48*(4), 815–822, doi:10.1016/0016-7037(84)90103-0.

Ni, Y., G. L. Foster, T. Bailey, T. Elliott, D. N. Schmidt, P. Pearson, B. Haley, and C. Coath (2007), A core top assessment of proxies for the ocean carbonate system in surface-dwelling foraminifers, *Paleoceanography*, *22*, PA3212, doi:10.1029/2006PA001337.

Penman, D. E. (2016), Silicate weathering and North Atlantic silica burial during the Paleocene-Eocene thermal maximum, *Geology*, *44*(9), 731–734, doi:10.1130/G37704.1.

Penman, D., B. Hönisch, R. E. Zeebe, E. Thomas, and J. C. Zachos (2014), Rapid and sustained surface ocean acidification during the Paleocene-Eocene Thermal Maximum, *Paleoceanography*, *29*, 1–13, doi:10.1002/2014PA002621.

Quintana Krupinski, N. B., A. D. Russell, D. K. Pak, and A. D. Paytan (2017), Core-top calibration of B/Ca in Pacific Ocean *Neogloboquadrina incompta* and *Globigerina bulloides* as a surface water carbonate system proxy, *Earth Planet. Sci. Lett.*, *466*, 139–151, doi:10.1016/j.epsl.2017.03.007.

Rink, S., M. Kühl, J. Bijma, and H. J. Spero (1998), Microsensor studies of photosynthesis and respiration in the symbiotic foraminifer *Orbulina universa*, *Mar. Biol.*, *131*(4), 583–595, doi:10.1007/s002270050350.

Rosenthal, Y., M. P. Field and R. M. Sherrell (1999), Precise determination of element/Calcium ratios in calcareous samples using sector-field inductively coupled plasma mass spectrometry, *Anal. Chem.*, *71*, 3248–3253, doi:10.1021/ac981410x.

Ruiz-Agudo, E., C. V. Putnis, M. Kowacz, M. Ortega-Huertas, and A. Putnis (2012), Boron incorporation into calcite during growth: Implications for the use of boron in carbonates as a pH proxy, *Earth Planet. Sci. Lett.*, *345-348*, 9–17, doi:10.1016/j.epsl.2012.06.032.

Russell, A. D., B. Hönisch, H. J. Spero, and D. W. Lea (2004), Effects of seawater carbonate ion concentration on shell U, Mg and Sr in cultured planktonic foraminifera, *Geochim. Cosmochim. Acta*, *68*(21), 4347–4361, doi:10.1016/j.gca.2004.03.013.

Salmon, K. H., P. Anand, P. F. Sexton, and M. Conte (2016), Calcification and growth processes in planktonic foraminifera complicate the use of B/Ca and U/Ca as carbonate chemistry proxies, *Earth Planet. Sci. Lett.*, *449*, 372–381, doi:10.1016/j.epsl.2016.05.016.

Spero, H. J. (1988), Ultrastructural examination of chamber morphogenesis and biomineralization in the planktonic foraminifer *Orbulina universa*, *Mar. Biol.*, *99*, 9–20, doi:10.1007/BF00644972.

Spero, H. J., S. M. Eggins, A. D. Russell, L. Vetter, M. R. Kilburn, and B. Hönisch (2015), Timing and mechanism for intratest Mg/Ca variability in a living planktic foraminifer, *Earth Planet. Sci. Lett.*, *409*, 32–42, doi:10.1016/j.epsl.2014.10.030.

Spero, H. J., and S. L. Parker (1985), Photosynthesis in the symbiotic planktonic foraminifer *Orbulina universa*, and its potential contribution to oceanic primary productivity, *J. Foramin. Res.*, *15*(4), 273–281, doi:10.2113/gsjfr.15.4.273.

Subhas, A. V., N. E. Rollins, W. M. Berelson, S. Dong, J. Erez, and J. F. Adkins (2015), A novel determination of calcite dissolution kinetics in seawater, *Geochim. Cosmochim. Acta*, *170*(C), 51–68, doi:10.1016/j.gca.2015.08.011.

Toyofuku, T., et al. (2017), Proton pumping accompanies calcification in foraminfera, *Nat. Commun.*, *8*, 14545, doi:10.1038/ncomms14145.
Uchikawa, J., D. E. Penman, J. C. Zachos, and R. E. Zeebe (2015), Experimental evidence for kinetic effects on B/Ca in synthetic calcite: Implications for potential B(OH)4− and B(OH)3 incorporation, *Geochim. Cosmochim. Acta*, *150*, 171–191, doi:10.1016/j.gca.2014.11.022.
Van Heuven, S., D. Pierrot, J. W. B. Rae, E. Lewis, and D. W. R. Wallace (2011), MATLAB Program Developed for CO2 System Calcuations, CO2sys, Carbon Dioxide Information Analysis Center, Oak Ridge Natl. Lab., Oak Ridge, Tenn.
Westerhold, T., U. Röhl, H. K. McCarren, and J. C. Zachos (2009), Latest on the absolute age of the Paleocene-Eocene Thermal Maximum (PETM): New insights from exact stratigraphic position of key ash layers +19 and −17, *Earth Planet. Sci. Lett.*, *287*, 412–419, doi:10.1016/j.epsl.2009.08.027.
York, D., N. Evensen, M. Martinez, and J. Delgado (2004), Unified equations for the slope, intercept, and standard errors of the best straight line, *Am. J. Physiol.*, *72*(3), 367, doi:10.1119/1.1632486.
Yu, J., H. Elderfield, and B. Hönisch (2007), B/Ca in planktonic foraminifera as a proxy for surface seawater pH, *Paleoceanography*, *22*, PA2202, doi:10.1029/2006PA001347.
Zachos, J., et al. (2005), Rapid acidification of the ocean during the Paleocene-Eocene Thermal Maximum, *Science*, *308*, 1611–1615, doi:10.1126/science.1109004.
Zeebe, R. E., and A. Sanyal (2002), Comparison of two potential strategies of planktonic foraminifera for house building: Mg^{2+} or H^{+} removal? *Geochim. Cosmochim. Acta*, *66*(7), 1159–1169, doi:10.1016/S0016-7037(01)00852-3.
Zeebe, R. E., J. C. Zachos, and G. R. Dickens (2009), Carbon dioxide forcing alone insufficient to explain Palaeocene-Eocene Thermal Maximum warming, *Nat. Geosci.*, *2*(8), 1–5, doi:10.1038/ngeo578.